Transcriptional responses of brain endothelium to *Plasmodium falciparum* patient-derived isolates *in vitro*

Caroline Askonas[1*], Janet Storm[2*], Grazia Camarda[2], Alister Craig[2#] and Arnab Pain[1#]

[1] Pathogen Genomics Laboratory, Bioscience Program, Biological and Environmental Sciences and Engineering (BESE), Division, King Abdullah University of Science and Technology, Thuwal, KSA

[2] Tropical Disease Biology, Liverpool School of Tropical Medicine, Pembroke Place, Liverpool L3 5QA, UK

[#] Address correspondence to: alister.craig@lstmed.ac.uk , arnab.pain@kaust.edu.sa

[*]Authors contributed equally to this work.

Abstract

A hallmark of cerebral malaria (CM) is sequestration of *Plasmodium falciparum* infected erythrocytes (IE) within the brain microvasculature. Binding of IE to endothelium reduces microvascular flow and combined with an inflammatory response perturbs endothelial barrier function, resulting in breakdown of the blood-brain barrier (BBB). Cytoadherence leads to activation of the endothelium and alters a range of cell processes affecting signalling pathways, receptor expression, coagulation, and disruption of BBB integrity. Here, we investigated whether CM derived parasites elicit differential effects on human brain microvascular endothelial cells (HBMECs), as compared to uncomplicated malaria (UM) derived parasites. Patient-derived IE from UM and CM clinical cases, as well as non-binding skeleton-binding protein 1 knockout parasites, were overlaid onto TNF-activated HBMECs. Gene expression analysis of endothelial responses was performed using probe-based assays of a panel of genes involved in inflammation, apoptosis, endothelial barrier function, and prostacyclin synthesis pathway. We observed a significant effect on endothelial transcriptional responses in the presence of IE, yet there was no significant correlation between HBMEC responses and type of clinical syndrome (UM or CM). Further, there was no correlation between HBMEC gene expression and both binding itself and level of IE binding to HBMEC, as we detected the same change in endothelial responses when employing both binding and non-binding parasites. Our results suggest that interaction of IE with endothelial cells in this co-culture model induce some endothelial responses that are independent of clinical origin and independent of the expression of the major variant antigen *Pf*EMP1 on the IE surface.

Keywords: cerebral malaria, cytoadherence, Plasmodium falciparum, HBMEC, endothelium, gene expression

Introduction

In spite of global efforts to reduce mortality and morbidity of malaria, an estimated 249 million cases and 608,000 deaths were reported in 2022, with the majority occurring in children under the age of five [1]. The majority of symptomatic infections result in mild febrile cases of uncomplicated malaria (UM), as severe disease only occurs in 1-2% of all cases [2]. Out of the eight *Plasmodium spp* that have been reported to cause either direct or zoonotic infection in humans, *P. falciparum* is considered a major driver of severe disease and mortality [3,4] . Cerebral malaria (CM) is a severe neurological complication of malaria infection that is a major cause of death, with mortality estimated between 15-25% and clinical manifestations including unarousable coma and seizures [5,6]. Mortality in paediatric CM is associated with brain swelling, which is considered to occur as a result of increased permeability of the blood-brain barrier (BBB) due to loss of

BBB function, leading to vasogenic oedema [6,7]. Continued study of the pathophysiology of CM is required to develop targeted treatment therapies.

It is evident that CM is a complex, multi-component disease requiring a multifactorial view of pathogenesis that considers the heterogeneous clinical manifestations of CM [8,9]. Sequestration of *P. falciparum*-infected erythrocytes (IE) to brain microvasculature is a hallmark of CM. Cytoadhesion of IE to the endothelium is mediated by *Plasmodium falciparum* erythrocyte membrane protein 1 (PfEMP1), a variable surface protein that is expressed by IE and contains an extracellular binding region [10]. This polymorphic protein is encoded by a group of approximately 60 *var* genes with monoallelic expression, and the composition of the extracellular region confers binding to various host receptors [11]. Several vascular surface proteins, in particular CD36, EPCR, and ICAM-1, may serve as IE adhesion receptors, and expression of these endothelial receptors varies between vascular locations and is modulated in part by cytokines, such as TNF and IFN [9,10,12,13]. EPCR is associated with severe malaria, as PfEMP1s containing EPCR binding domains have been linked to brain swelling in paediatric CM [14-17]. While ICAM-1 mediates cytoadhesion related to sequestration in the brain [13-15], its direct role in the pathology of CM is less clear. However, research has demonstrated that a subset of EPCR-binding parasites has the ability to bind ICAM-1and that expression of these dual binders has been associated with CM in patients [15,18,19]. Cytoadherence alters a range of endothelial cell processes and leads to the activation of endothelium as well as reducing microvascular flow. Accumulation of IE causes vessel occlusion and generates microenvironments where both parasite factors and soluble erythrocytic content accumulate after IE rupture [8,20]. Ultimately, the contributions of microvascular obstruction and endothelial dysfunction lead to the disruption and breakdown of the BBB [5,8,9,17].

Although IE derived from malaria patients have exhibited different binding phenotypes, most studies employ well characterized laboratory strains to investigate cytoadherence and interaction of different PfEMP1 variants to brain endothelial cells [19,21-24]. Separate investigations have highlighted the divergent effect of both TNF stimulation and IE cytoadhesion on endothelial transcriptional responses and the pathways they induce [23,25]. IE isolated from peripheral blood of UM and CM patients have been used to study cytoadherence to human brain microvascular endothelial cells (HBMEC). It was found that IE isolated from CM patients exhibit differential binding capacities to TNF-activated brain endothelium *in vitro*, as they were associated with increased adhesion [26]. Further study employing patient-derived isolates is needed to elucidate the impact of parasite cytoadhesion on the brain microvasculature in association with different disease outcomes.

The aim of this study is to investigate whether CM-derived IE elicit differential effects on HBMEC as compared to UM-derived isolates. An *in vitro* co-culture model of cytoadherence was employed wherein patient-derived IE isolates were overlayed onto TNF-activated HBMEC and the relative gene expression of HBMEC after incubation with either RBC or IE for a panel of genes was assessed. A study utilizing two *P. falciparum* lab strains with different binding capacities to HBMEC found that different PfEMP1-expressing variants induced divergent endothelial transcriptional responses during cytoadherence [25]. Differentially expressed genes (DEGs) were identified in HBMEC in pathways involved in the pathology of severe malaria, such as inflammation, apoptosis, and barrier integrity. From this list of DEGs, a panel of genes was compiled, and gene expression was investigated by qPCR using the Fluidigm DELTAgene assays system. First, the relative gene expression of HBMEC after exposure to control RBC or IE for combined UM and CM-derived isolates was compared, followed by comparing the expression data between clinical type. We observed variation in endothelial transcriptional responses to individual patient-derived IE as compared to RBC, but these responses did not show a significant differential effect between the UM or CM-derived isolates. It was assessed whether the HBMEC relative gene expression after co-culture was correlated with the binding avidity of the parasite isolates, but a significant relationship was not observed. Our data confirm that IE have a profound effect on endothelial transcription that is specific to the presence of the *P. falciparum* parasites in the erythrocyte. However, we did not observe effects that were associated with disease severity with the panel of genes used in this study.

Materials and Methods

Culture of Endothelial Cells

Primary HBMEC were obtained from Cell Systems, USA (ACBRI 376) and cultured in Endothelial Cell Growth Medium 2 (EGM2) media (C-22111, Promocell) supplemented with 2% foetal calf serum (FCS), 5 ng/mL epidermal growth factor (EGF), 10 ng/mL basic fibroblast growth factor, 20 ng/mL Long R3 IGF-1, 0.5 ng/mL VEGF 165, 1 µg/mL ascorbic acid, 22.3 µg/mL heparin, and 0.2 µg/mL hydrocortisone from the supplement pack (C-39211, Promocell) in a 5% CO2 incubator at 37°C. For endothelial cells to adhere to the surface, flasks were coated with attachment factor (10308363, Gibco). Cells were passaged using Accutase solution (A6964, Sigma Aldrich), following manufacturer instructions. The receptor expression of HBMEC was characterised by flow cytometry as described by Storm et al [26].

127 **Culture of *P. falciparum* Parasites**

128 Patient-derived *P. falciparum* parasites were isolated from peripheral blood from paediatric malaria cases
129 recruited at the Queen Elizabeth Central Hospital, Blantyre, Malawi with ethical approval from the College
130 of Medicine, University of Malawi and LSTM, as described in Storm et al [26]. Four UM and four CM patient-
131 derived isolates were selected based on their differential cytoadherence profile to HBMEC and human
132 dermal microvascular endothelial cells and their ability to establish in continuous culture (Figure 3). After
133 isolation from blood, limited IE could be cryopreserved, especially for CM isolates, and only a maximum
134 of 150 µl IE could be frozen. Establishing the isolates as a continuous culture, expanding the cultures to
135 generate more stabilates, and subsequently have 65 ml of culture volume at 2% HCT for the co-cultures
136 requires a considerable amount of time. Therefore, co-cultures were performed after at least 21 days in
137 culture (DIC). The total DIC for the patient-derived parasite isolates for co-culture 1 and 2, respectively,
138 were UM1: 24 and 43, UM2: 21 and 32, UM3: 31 and 42, UM4: 24 and 25, CM1: 29 and 29, CM2: 35 and
139 44, CM3: 49 and 59, and CM4: 29 and 41. The skeleton-binding protein knockout (SBP1-KO) lab strain
140 was obtained from A.G. Maier and cultured in the presence of 4 nM WR99210 [27].

141

142 The IE were cultivated at 2% haematocrit in O+ human erythrocytes and grown at 37°C in multiple 25cm^2
143 tissue culture flasks (T25) filled with a gas mixture of 96% nitrogen, 3% carbon dioxide, and 1% oxygen.
144 The duration of parasite culturing was isolate dependent, as different lengths of continuous culture were
145 required to generate enough material to perform the experiments, ranging from 21-60 DIC. IE were
146 maintained in complete RPMI 1640 medium with 11 mM glucose and 0.2% sodium bicarbonate (R-0883,
147 Sigma) supplemented with 5% human serum, 0.25% Albumax II (11021029, ThermoFisher Scientific), 30
148 mM of HEPES (15630122, Gibco), 2 mM L-glutamine (G-7513, Sigma), 25 ng/mL gentamicin sulphate
149 solution (G-1271, Sigma), and 0.11 mM hypoxanthine (H9636, Sigma) pH 7.4. Parasite growth was
150 monitored using Giemsa staining (1092040500, Merck), and IE were passaged to maintain 2-5%
151 parasitaemia. Mixed-staged cultures were synchronized for ring stages using a 5% D-sorbitol solution
152 (S3889, Sigma), and IE at trophozoite stage were used for the *in vitro* co-culture studies with HBMEC. EC
153 cultures, parasite lines, culture media, and washed RBCs were monitored for mycoplasma contamination
154 using MycoBlue™ Mycoplasma Detector (Vazyme, D101-02).

155

156 **Co-culture of HBMEC and IE**

157 HBMEC at passage 5-8 were cultured until 90% confluency in T25 flasks. One day prior to co-culture,
158 HBMEC were seeded in 12-well plates at a density of 50,000 cells/cm^2 (for 3.8 cm^2 wells, this is equivalent
159 to total of 190,000 cells) in the morning and stimulated overnight with 10 ng/mL TNF (PHC3015,

160 Invitrogen). The RBC control was prepared by culturing a 2% haematocrit suspension in RPMI medium
161 overnight. On the day of the co-culture, the supernatant was removed from the HBMEC and replaced with
162 EGM2 media without heparin and hydrocortisone (EGM2min media) 2 hours prior to co-culture. IE were
163 enriched for mature stages by layering onto a 0.7% gelatine solution and incubation at 37°C for 45-60
164 minutes and after enrichment, the haematocrit and parasitaemia were calculated and IE suspensions were
165 prepared to an average parasitaemia of 30% (parasitaemia ranged from 20-40%, depending on enrichment
166 properties of the isolates) at 1% haematocrit in EGM2min media.

167

168 The RBC control was also subjected to gelatine treatment and a suspension at 1% haematocrit in EGM2min
169 media was prepared. EGM2min medium was used to maintain healthy HBMEC and did not affect parasite
170 viability in the 6-hour co-culture, but parasite development seemed delayed, as assessed by microscopy.
171 Medium was removed from the HBMEC, and 700 µl IE or RBC suspension were overlayed onto HBMEC
172 for 6 hours in a 5% CO2 incubator at 37°C, as well as EGM2min medium as an additional control. 700 µL
173 of 30% parasitaemia at 1% haematocrit is equivalent to $2.1x10^7$ IE and addition of the IE suspension to
174 HBMEC is equivalent to a ratio of 110 IE/HBMEC. A 0-hour control with EGM2min medium was used to
175 compare with the 6-hour time points. Control samples were generated by overnight incubation of HBMEC
176 with either 10 ng/mL of TNF, or 1 ng/mL IL-1 beta (579402, BioLegend) and compared to EGM2min
177 medium, for which samples were collected directly after stimulation.

178

179 At each time point, the co-culture medium was removed, and the HBMEC were washed once with
180 EGM2min medium to remove unbound IE or uninfected RBC. Cells were directly lysed in the well using
181 350 µL of lysing solution (1% 2-mercaptoethanol in Buffer RLT; RNeasy Mini Kit, 74106, Qiagen) by
182 pipetting over the well. The lysates were collected into a 1.5mL sterile tube, vortexed, and stored at -80°C
183 until RNA extraction. Two independent co-culture experiments were performed for each patient isolate and
184 SBP1-KO.

185

186 In parallel to the co-culture experiments, activation of HBMEC after overnight incubation with TNF was
187 assessed. One day prior to co-culture, HBMEC were plated onto 24-well plates at a density of 50,000
188 cells/cm^2. The HBMEC were incubated overnight with either media alone or media containing 10 ng/mL
189 of TNF. Cells were detached with Accutase, collected in PBS + 1% FBS and stained for ICAM-1 expression
190 on the endothelial cell surface using APC anti-human CD54 antibody (353111, Biolegend). Flow cytometry
191 analysis was performed and confirmed that ICAM-1 expression was upregulated following overnight
192 stimulation with TNF in each of the co-culture experiments.

193

194 **RNA Extraction and Quality Assessment**

195 Frozen HBMEC lysates were placed in a 37°C water bath until thawed and salts dissolved. Total RNA was
196 purified using the RNeasy Mini Kit (74106, Qiagen) following the manufacturer's instructions using steps
197 4 -10 of the "Purification of Total RNA from Animal Cells using Spin Technology" protocol. RNA was
198 eluted in 50 µL of RNase-free water.

199

200 The RNA concentration of each sample was quantified using a Qubit fluorometer and the RNA High
201 Sensitivity assays (Q32852, Invitrogen), following manufacturer instructions. The quality of the RNA
202 samples was assessed using an Agilent 2100 Bioanalyzer (RNA 6000 Nano Kit, 5067-1511, Agilent
203 technologies) following manufacturer instructions. The RIN for all samples was between 9.4-10, indicating
204 high quality RNA.

205

206 **Gene Expression Assays using the Fluidigm System and Calculations**

207 Gene expression qPCR assays were conducted on the extracted RNA for a panel of 49 genes that include
208 pathways pertaining to inflammation, apoptosis, endothelial barrier function, and prostacyclin synthesis
209 (listed in Supplementary Table 1). In short, cDNA was prepared with reverse transcription before pre-
210 amplification (13-cycles) and clean-up of the reactions using Exonuclease 1, following the manufacturer
211 protocols (100-6472 B1, PN 100-5875 C1) and reagents (Fluidigm,100-6297; Fluidigm, 100-5580; New
212 England Biolabs, M0293S; TEKnova, 10221). Real-time PCR data was collected using the Biomark HD
213 system with a 96.96 IFC chip using Fluidigm Delta-Gene Assays on the pre-amplified cDNA. The
214 manufacturing protocol was followed for use of the Biomark HD system (PN 100-9792 A1) using the
215 reagents specified for preparing samples (Biorad, 172-5211; Fluidigm, 100-7609)) and assays (Fluidigm
216 100-7611; TEKnova, 10221). Technical replicates were performed for each sample, and Ct values were
217 obtained as the throughput of the real-time data. The primers for the gene panel were proprietarily designed,
218 prepared, and tested by Fluidigm.

219

220 Relative gene expression was calculated using the $2^{-\Delta\Delta Ct}$ method as previously described [28] using GAPDH
221 as the endogenous control (ΔCt) and the 6-hour EGM2min media-only sample as the normalization controls
222 (ΔΔCt). In this way, the exponential fold changes (FCs, $2^{-\Delta\Delta Ct}$) in the target genes are calculated as
223 normalized to the GAPDH internal control and relative to the expression of the HBMEC-media only at the
224 6-hour time point. For each target gene, the gene expression of HBMEC incubated with EGM2min media

225 at 6-hours is equal to 1 (baseline). Therefore, an FC>1 indicates increased relative gene expression and an
226 FC <1 indicates decreased relative gene expression for the experimental samples. FCs were calculated for
227 each technical triplicate of each sample for each experiment. To compare relative gene expression of
228 HBMEC after incubation with various groups (e.g., RBCs, UM-derived parasite isolates, CM-derived
229 parasites isolates, or combined IE), the mean, standard error of the mean (SEM), and confidence intervals
230 for each group were calculated from the technical triplicates of each sample for each independent
231 experiment. Either two-tailed, unpaired T-tests or Welch's T-test were then performed to compare the
232 relative gene expression between various corresponding groups. Additionally, a paired analysis was
233 performed wherein the HBMEC-IE relative gene expression for each parasite isolate was compared to the
234 corresponding HBMEC-RBC relative gene expression, for both experiments. For this analysis, the target
235 FCs were calculated as normalized to GAPDH and relative to the corresponding experimental 6-hour
236 EGM2min media, and the mean and SD were determined from the technical triplicates for each sample.
237 Both independent experiments for all isolates were performed for a 6-hour timepoint.

238

239 **Binding of Parasite Isolates to HBMEC under Flow Conditions**

240 The binding assay was performed using the Cellix microfluidics system as previously described [26,29].
241 Briefly, HBMEC or HDMEC were stimulated overnight with 10 ng/ml TNF, detached, and seeded in
242 attachment factor coated Vena8 biochips (Cellix). When cells formed a confluent monolayer, an IE
243 suspension of 2% parasitaemia and 5% haematocrit in binding buffer (RPMI 1640 with 25 mM HEPES, 11
244 mM glucose, 2 mM glutamine, pH 7.2) was flowed through for 5 minutes at 37 °C at a shear stress of 0.4
245 dyne/cm2. After a washing step, bound IE were counted by microscopy in 15 areas throughout the biochip
246 and the mean IE/mm^2 EC cell surface calculated.

247

248 **Statistical Analysis**

249 Statistical analyses were performed on Prism 9 (Version 9.5.1, GraphPad Software). The exact statistical
250 tests, along with the levels of significance, are detailed in the figure legends.

251

252 **Data Availability**

253 Data will be made publicly available upon publication.

254

255

256 **Results**

257 **Expression of intermediates involved in maintaining vascular barrier integrity is increased in**
258 **HBMEC in response to patient-derived *P. falciparum* parasites.**

259 To investigate endothelial responses to the patient-derived parasite isolates, we compared the relative gene
260 expression of TNF-activated HBMEC after six-hour exposure to either RBC or IE derived from patients
261 with clinically defined UM or CM. Additional media-only samples were collected to be used as
262 normalization controls in the relative gene expression calculations.

263

264 The relative gene expression of 49 target genes was analysed by grouping HBMEC samples by clinical type
265 of the patient isolates, either HBMEC-UM or HBMEC-CM, and comparing them to the corresponding
266 HBMEC-RBC control. Gene expression was calculated for HBMEC-UM, HBMEC-CM, and
267 corresponding HBMEC-RBC by determining the mean FC±SEMs for each group relative to the
268 corresponding 6-hour EGM2min media controls in each of the two independent experiments. Welch's t-
269 tests were performed to compare the relative gene expression of the HBMEC-IEs to their corresponding
270 HBMEC-RBC controls, and the mean FC±SEMs are reported in Supplementary Table 1.

271

272 Differential gene expression was observed in HBMEC in the presence of IE compared to the corresponding
273 RBC control for a number of genes, and several were selected for further study due to their relatively
274 increased expression (FC > 1.7), as well as the biological processes they are involved in. These genes
275 encode: B-cell lymphoma 2-related protein A1 (*BCL2A1*), cytochrome P450 family 1 subfamily A member
276 1(*CYP1A1*), Krüppel-like factor 2 (*KLF2*), Krüppel-like factor 4 (*KLF4*), prostacyclin synthase (*PTGIS*),
277 and prostaglandin-endoperoxide synthase 2 (*PTGS2*).

278

279 A significant increase in expression of *BL2A1*, *CYP1A1*, *KLF2*, *KLF4*, *PTGIS*, and *PTGS2* was observed
280 for HBMEC after co-culture with both clinical isolate types as compared to the RBC controls (Figure 1,
281 Supplementary Table 1). The mean HBMEC gene expression was compared in two ways: grouping by
282 clinical syndrome compared to the corresponding RBC and grouping by combining all IE samples
283 compared to the corresponding RBC. The results for each gene are shown in Figure 1, with a sub-figure
284 showing the combined data for HBMEC-RBC and HBMEC-IE co-culture, with paired data points from the
285 same experiment joined by a line. This allows visual verification of increased gene expression within each
286 experiment, which corresponds to the increase in gene expression observed when samples are grouped by
287 clinical type.

288

289 To validate the observed changes in gene expression, we assessed whether the Fluidigm panel would detect
290 gene upregulation after incubating HBMEC overnight with known stimuli, IL-1beta and TNF, and
291 comparing the relative gene expression with a media control (Supplementary Table 2). Indeed, incubation
292 with these stimuli resulted in upregulation of HBMEC expression in the majority of tested genes, with large
293 fold changes observed in both treatment groups for the following (IL-1beta and TNF, respectively): *CXCL3*
294 (1305 and 862), *ICAM1* (16 and 25), *PTGS2* (30 and 16), *SELE* (1305 and 862), and *VCAM1* (548 and 873).

295

296 Previous studies have demonstrated that TNF differentially regulates transcriptional effects on brain
297 endothelial cells [23,30], such as upregulated expression of *BCL2A1* in vascular endothelial cells [31], 0-hour
298 data was collected to assess if the observed HBMEC FC expression was due to either activation with TNF
299 or the effect of IE. To demonstrate the impact of TNF withdrawal, the relative gene expression of activated
300 HBMEC after 2-hours (0-hour timepoint) and 8-hours (6-hour timepoint) incubation with media were
301 compared for representative samples (Supplementary Figure 1). There was significant reduction of relative
302 FC levels of *KLF4*, *PTGS2*, *ICAM-1*, *VCAM-1*, and an observed reduction in *BCL2A1* in HBMEC after
303 withdrawal of TNF after 8 hours. These findings show that the differences in relative gene expression
304 observed after co-culture are not artifacts of overnight TNF stimulation of the HBMEC.

305

306 ***P. falciparum* parasites derived from uncomplicated or cerebral malaria cases do not induce divergent**
307 **HBMEC responses for the genes tested.**

308 To determine whether the observed effect on HBMEC responses to the patient-derived IE was specific to
309 the clinical syndrome, the effect of RBCs on HBMEC was normalized. To take into account variation in
310 the RBCs for each experiment, gene expression FCs ($2^{-\Delta\Delta Ct}$) were calculated relative to the corresponding
311 6-hour HBMEC-RBC sample, which was used as the normalization control (ΔΔCt). Mean gene FCs were
312 calculated for each clinical isolate type (HBMEC-UM and HBMEC-CM) using the triplicates of all the
313 experimental samples. Unpaired t-tests were performed to compare the mean relative gene expression of
314 HBMEC-UM to HBMEC-CM (Figure 2). Apart from *PTGIS*, there was no differential effect on HBMEC
315 transcriptional responses when comparing UM and CM-derived isolates.

316

317 The isolates chosen for this study were from a panel of patient-derived *P. falciparum* parasites, isolated
318 from paediatric uncomplicated and cerebral malaria cases in Malawi as described in Storm et al [26]. During
319 extended periods of culture, and when establishing *in vitro P. falciparum* culture lines from patient parasite
320 isolates, the *var* gene transcription profiles may change which could affect phenotypic changes, such as

321 binding to HBMEC [32,33]. To establish the isolates in culture and expand the volume to sufficient levels, the
322 experiments were carried out after culturing the IE for 21-60 days. To determine if their adherence to
323 HBMEC had changed due to *var* gene switching over time [32,33], binding assays under flow conditions were
324 performed as close to the length of culture time (days in culture, DIC) for each co-culture experiment
325 (Figure 3). Compared to their initial binding phenotype, all isolates showed altered binding to HBMEC.
326 UM1, UM3, UM4, CM2 and CM3 increased their binding after various days in culture, with some variation
327 between the two sets of DIC, and UM2 and CM4 decreased their binding. The SBP1-KO strain does not
328 bind to HBMECs.

329

330 Using data from both experiments, the binding capacities of the isolates were then correlated with the mean
331 gene expression (FC calculated using the 6-hour RBC as the normalization control) of HBMEC following
332 co-culture with IE using Spearman's correlation. These calculations were performed for the entire gene
333 panel by grouping the data per experiment, and representative plots for *KLF4*, *PTGIS*, and *PTGS2* are
334 presented in Supplementary Figures 2A and 2B for both experiments. After co-culture, there was no
335 observed significant correlation between the binding avidity of the parasites and the HBMEC gene
336 expression.

337

338 **Observed differential effects of *P. falciparum* parasites on HBMEC responses is not solely due to**
339 **binding.**

340 To further investigate whether the observed differential effects on HBMEC transcriptional responses were
341 due to the direct interaction between the IE and the surface of HBMEC, two co-culture experiments were
342 performed using the non-binding parasite strain, skeleton-binding protein knockout parasites (SBP1-KO).
343 These parasites are unable to traffic *Pf*EMP1 to the infected erythrocyte surface, and therefore, they are
344 unable to bind to endothelium [27,34], verified by using flow binding assays to HBMEC (Figure 3). The mean
345 relative gene expression was calculated for the technical and biological replicates. Welch's t-tests were
346 performed to compare the relative FC of the HBMEC-SBP1KO parasites and the HBMEC-RBC controls
347 (Supplementary Table 3). The relative gene expression of the HBMEC incubated with the binding patient-
348 derived parasites (HBMEC-binding IE), and non-binding SBP1-KO parasites, as compared to the HBMEC-
349 RBC controls, are shown in Figure 4 for *BCL2A1*, *CYP1A1*, *KLF2*, *KLF4*, *PTGIS*, and *PTGS2*.

350

351 Even though similar effects were observed from the SBP1-KO parasites on HBMEC transcriptional
352 response when compared to the patient-derived isolates for these genes, the magnitude of the effect is not

always the same between HBMEC-SBP1-KO and the HBMEC-binding IE. The relative FC of the HBMEC-binding parasites and the HBMEC-SBP1KO parasites were compared (Supplementary Table 4), and out of the genes presented in Figure 4, there were significant differences between the two groups for *BCL2A1*, *KLF4*, and *PTGS2*. There is large variation in responses within the binding-IE group, likely due to the expression of different *Pf*EMP1variants, suggesting that more than one process is occurring, one of which is adhesion independent. The observed differential effect on HBMEC transcriptional responses is related to parasite-infected RBC, but not exclusively binding via *Pf*EMP1.

As shown in Figure 3, differences in cytoadhesion of the patient-derived isolates to HBMEC were measured after culturing. To determine PfEMP1 domains expressed, *var* genotyping by qPCR was used and the data compared to the qPCR data from when the parasites were isolated from the patients (Supplementary Table 5) [26]. Primer sets detecting multiple group A and A/B var domains were used, with the CIDRα1 domains predicting PfEMP1 binding to EPCR and the DBLβ domains predicting binding to ICAM-1, both these receptors are expressed on HBMEC. A transcription unit of at least 32 denotes a transcription level equal to the endogenous genes seryl-tRNA synthetase and aldolase, used to normalise the data. High transcript levels of the initial DBLα domains remained for UM4 and CM1 after 26 and 29 DIC, respectively, while the levels decreased substantially for CM2 (43 DIC) and CM4 (33 DIC), indicative for *var* gene switching. CM1 seemed to maintain similar transcripts levels for most of the var domains.

Determination of prostaglandin endoperoxide synthase 2 and prostacyclin production in HBMEC-IE co-cultures

HBMEC-IE co-culture activates the prostacyclin pathway as shown for *PTGIS* and *PTGS2* in the Fluidigm results (Figure 1). Whether that results in increased concentrations of its end-product prostacyclin or the intermediate PTGS2 was determined by ELISA. Prostacyclin is secreted but has a short half-life, therefore its hydrolysis product, 6-keto prostaglandin F1α (6-keto PGF1α) was measured in co-culture medium of HBMEC-IE and compared with their respective HBMEC-RBC controls (Supplementary Table 6 and Supplementary Figure 3). Overall, there is some variability between the experiments, but no significant differences were detected between the co-cultures. However, the positive controls, HBMEC activated with TNF or thrombin, did increase 6-keto PGF1α concentrations. PTGS2 was detected in HBMEC cell lysate after co-culture and calculated as ng PTGS2 per mg total lysate protein (Supplementary Table 6). Overall, there was a small decrease in PTGS2 generation after HBMEC-IE co-culture, but only significant for CM1 (experiment 9) and CM4 (experiment 6).

386 **Production of cytokines by HBMEC-IE co-cultures**

387 To determine if the production of cytokines or chemokines by HBMEC was altered following co-culture, a
388 multiplex panel of 41 secreted cytokines and chemokines was used. The multiplex was performed at an
389 early stage of the study and only included 6-hour co-culture medium of five isolates and two lab strains
390 IT4var14 and IT4var37 in one experiment. These lab strains were included because they were used in
391 previous co-culture experiments [25]. Concentrations higher than 5 pg/ml were detected for 13 cytokines and
392 only a few of these were significantly increased after co-culture with IE, compared to co-culture with their
393 respective RBC control (Supplementary Table 7). CM4, the isolate with the highest binding to HBMEC,
394 significantly increased production of IL-6, IL-8 and IP-10, GRO, G-CSF and GM-CSF. Although at low
395 levels, IFNγ was increased two to ten-fold by co-culture with the patient isolates, but not significantly by
396 the lab strains IT4var14 and IT4var37. A positive control of TNF-activated HBMEC was included to
397 produce high enough levels of cytokines to be measured, and for 10 analytes these were at least 10-fold
398 higher than medium only. Notably, TNF was still detectable at ~11 ng/ml in the culture medium after 16
399 hours.

400

401 **Effect of IE co-culture on HBMEC barrier integrity**

402 Although the cytoadherence phenotype of the isolates to HBMEC altered during culture, there are still
403 detectable differences, especially between CM2 and CM4 with low and high binding, respectively. Whether
404 differential binding capacity of the patient isolates could affect HBMEC barrier function was determined
405 by trans endothelial electrical resistance (TEER). Barrier function increased slightly by adding RBC,
406 irrespective if they were infected or not (Supplementary Figure 4B). Thrombin induces a rapid decrease in
407 barrier function, which recovers within 2 hours. The presence of RBC and IE partly protected against this
408 effect by reducing the maximum decrease (Supplementary Figures 4C and 4E) and the rate of recovery,
409 determined by the area under the curve (AUC) (Supplementary Figures 4D and 4F). RBC and IE all
410 significantly reduced thrombin-induced decrease in barrier function compared to medium, but IE was not
411 significantly different to RBC. The recovery rate was more rapid with a significantly reduced AUC for
412 RBC, 5%, 10%, and 30% IE compared to medium with a trend of more rapid recovery with increasing
413 parasitaemia. The AUC for SBP1-KO at the different parasitaemias were similar and not distinct compared
414 to medium, but all significantly different than the AUC of 30% IE, which had the smallest AUC at 13.5. No
415 differences between the individual UM and CM-derived isolates could be detected.

416

417

418

419 **Discussion**

420 A view of CM pathology has emerged in recent years that proposes dysregulation of coagulation pathways,
421 inflammation, release of parasite factors from mature IE, and sequestration of IE in the vasculature all
422 contribute to endothelial dysfunction and-breakdown of the BBB [8,9,35]. Cytoadhesion of IE to endothelial
423 cells is one of the events in a multi-step process leading to localized accumulation of both IE and RBC, as
424 well as rupture and release of parasite and intercellular erythrocyte components and soluble factors,
425 resulting in activation of the endothelium and immune responses, compromising BBB integrity [20,36].

426

427 In the present study, HBMEC responses to clinically derived parasites isolates from UM and CM patients
428 were investigated by employing an *in vitro* co-culture model of cytoadhesion. We found that IE from both
429 UM and CM-derived isolates have differential effects on the HBMEC transcriptional response as compared
430 to RBCs for 28 genes (Supplementary Table 1 and Figure 1), but there was no difference when comparing
431 UM with CM patient-derived isolates (Figure 2). The UM and CM-derived isolates were selected for this
432 study based on their diverse binding capacities to HBMEC and HDMEC from a previous study [26], and their
433 ability to be established in continuous culture to provide sufficient material for repeat experiments.
434 Adapting *P. falciparum* patient-derived isolates to *in-vitro* culture requires considerable time, and thus *var*
435 gene switching is likely to occur [32,37], which was the case for the CM and UM isolates, as detected by qPCR
436 (Supplementary Table 5). This resulted in altered binding profiles to TNF-stimulated HBMEC with less
437 distinction between the isolates compared to that seen at the time of isolation from patients, with exceptions
438 of CM2 and CM4, which still had relatively low and high binding to HBMEC, respectively (Figure 3).
439 Binding to HDMEC was not determined in this work for the cultured-adapted isolates, as the co-cultures
440 were only performed with HBMEC. Despite the variability in binding profiles, we observed important
441 differences in the HBMEC transcriptional response to IE compared to RBC in our *in vitro* model, supporting
442 a role for PfEMP1 in shaping the endothelial response to sequestration.

443

444 Comparing the binding capacity of each isolate to the relative gene expression of HBMEC after 6-hours
445 co-culture detected no significant correlation between the parasites' propensity to bind and the HBMEC
446 gene expression of *PTGIS*, *PTGS2* or *KL4* (Supplementary Figure 2). Furthermore, experiments performed
447 using the SBP1-KO parasite line revealed that there were no differences in the HBMEC responses to
448 binding and non-binding IE for these genes (Supplementary Table 3), yet there was a significant difference
449 in the magnitude of these responses between these two groups for 30 genes (Supplementary Table 4). SBP1-
450 KO parasites do not cytoadhere to HBMEC as they are unable to traffic PfEMP1 to the surface, although
451 they maintain both Maurer's cleft and knob morphology and the expression of other Maurer's cleft-

452 associated proteins essential for tracking and IE surface changes, such as KAHRP, MAHRP, REX, PfEMP3,
453 and Pf332 [27,34]. RIFINs and STEVORs are proteins that are expressed on the surface of IE that are involved
454 in cytoadherence to RBC (rosetting) and immune cells [38], and their trafficking and expression is maintained
455 in SBP1-KO parasites [39]. Possemiers et al investigated sequestration-deficiency in experimental
456 *Plasmodium berghei* malaria-associated acute respiratory distress syndrome, and they observed endothelial
457 activation in SBP1-KO infected mice to the same level as wild type at eight days post infection in the lungs
458 [40]. Overall, SBP1-KO IE maintain an altered surface, including knobs, and can interact with HBMEC
459 differently compared to RBC. Our findings suggest that the interaction between HBMEC and IE via
460 PfEMP1 is not the only driver and that the observed differences in HBMEC relative gene expression are
461 also related to contact with intact parasitised RBC.

462

463 We observed upregulation in relative gene expression of HBMEC after incubation with IE in a panel of
464 genes, particularly in genes involved in apoptosis and the regulation of inflammation and endothelial
465 integrity. Overall, the fold change expression levels were relatively low, except for the ones highlighted for
466 further study and discussion. *BCL2A1* is a member of the pro-survival sub-family of BCL2 proteins that
467 include both pro- and anti-apoptotic regulators, and it encodes a protein that reduces the release of pro-
468 apoptotic cytochrome C and blocks caspase activation through inhibition of caspace9 [41,42]. Expression of
469 *BCL2A1* is upregulated in vascular endothelial cells by the inflammatory cytokines TNF and IL-1beta [31,43].
470 *BCL2A1* expression was increased and a more robust *BCL2A1* expression was observed in HBMEC co-
471 cultured with binding IE, as compared to non-binding SBP1-KO (Supplementary Table 3). Perhaps
472 expression of *BLC2A1* early during an infection represents the balance between protection and pathology
473 and demonstrates the temporal kinetics in this complicated system. KLF2 and KLF4 are transcription
474 factors that have been shown to directly regulate endothelial function and integrity in vascular endothelium
475 and to protect against endothelial dysfunction, both *in vitro* and in murine models, and their expression is
476 modulated by both changes in laminar sheer flow or stress and pro-inflammatory stimuli [44-49].
477 Overexpression of *KLF2* and *KLF4* affect coagulation and inflammatory pathways by inducing expression
478 and activity of endothelial nitric oxide synthase and thrombomodulin [44-46,50,51], while simultaneously
479 inhibiting expression of adhesion molecules E-selectin, ICAM-1, and VCAM-1 [45]. We observed significant
480 upregulation in relative gene expression of both *KLF2* and *KLF4* in HBMEC incubated with IE. CYP1A1,
481 PTGIS, and PTGS2 are involved in lipid metabolism, including the biosynthesis of prostacyclin, which has
482 roles as an inflammatory mediator and a potent vasodilator [52,53]. CYP1A1 is a member of the cytochrome
483 P450 enzyme family that metabolizes a range of substrates, including arachidonic acid [54]. Both PTGIS and
484 PTGS2 are enzymes involved in the biosynthesis of prostacyclin, a bioactive lipid that is produced by
485 vascular endothelial cells and that plays a role in regulation of endothelial inflammation and apoptosis [52].

486 A recent study demonstrated differential gene expression of *CYP1A1*, *PTGIS*, and *PTGS2* between HBMEC
487 incubated with two parasite lines that expressed different *Pf*EMP1s [25]. As reported in that study, we
488 observed evaluated levels of CYP1A1 induced by both IE and RBC controls. Despite observing
489 transcriptional upregulation of *PTGIS* and *PTGS2*, FC±SEM of 2.05±0.24 and 4.92±0.26 respectively
490 (Supplementary Table 3), this did not seem to translate into detection of PTGS2 protein or 6-keto PGF1α
491 (prostacyclin's stable hydrolysis product) in HBMEC lysate and co-culture supernatant, respectively
492 (Supplementary Table 6). PTGS2 is intracellularly localised, and expression in cell lysates is usually
493 detected by Western blot. An ELISA was employed to quantify PTGS2 concentrations in multiple samples.
494 Unfortunately, the usability of the ELISA kit was questionable, as the positive control, stimulation with
495 TNF, did not result in increased PTGS2 production, and detection of PTGS2 was not pursued further. 6-
496 keto PGF1α is secreted, and larger amounts were produced upon stimulation with TNF and thrombin, but
497 overall, no significant increase in production was detected for the HBMEC-IE co-cultures compared to their
498 respective HBMEC-RBC co-cultures. Overall, our findings provide additional evidence that IE regulate
499 brain ECs and that these effects are not only due directly to binding.

500

501 Previous studies have investigated the effects of IE on endothelial responses *in vitro*. An investigation by
502 Zuniga et al examined how TNF and IE differently affected transcriptional responses and barrier integrity
503 in brain endothelial cells. Their work highlighted that TNF and IE lysates induce distinct transcriptional
504 profiles, with TNF associated with induction of endothelial activation while IE lysate contributed
505 considerably to endothelial barrier disruption, yet overlap in genes associated with inflammation, including
506 induction of PTGS2, were detected [23]. Howard et al adapted a 3D perfusion human brain microvessel model
507 to evaluate the brain endothelial responses to perfusion with TNF and at different stages of parasite
508 maturation. This study found that treatment of brain microvessels with TNF induced an inflammatory
509 phenotype, while EPCR-binding parasites caused localised barrier damage, and induced unique stress
510 response pathways associated with metal toxicity and oxidative stress [30]. In concordance with Zuniga et al
511 and Howard et al [23,30], we observed that a group of inflammatory associated genes are upregulated in
512 HBMEC by exposure to patient-derived IE and this effect is independent of TNF treatment. This
513 upregulation in HBMEC relative gene expression was detected after 6-hours incubation with trophozoite-
514 stage IE, in contrast to studies that used schizont-stage IE or IE lysates for longer periods ranging from 6,
515 9, 12, and 24 hours [23,30]. In contrast to these studies [23,30,55], we utilised trophozoite-IE prepared in EGM2min
516 medium for a 6-hour incubation period. This medium maintains HBMEC over the time course, but affects
517 the progress of IE, as they barely develop beyond the trophozoite stage. In our study, we detect HBMEC
518 effects at early stages of sequestration where IE are still in contact with the endothelium, as opposed to

519 effects attributed to parasite material and ruptured IE. An extended co-culture time frame would have
520 allowed us to observe other, perhaps larger, effects on HBMEC transcription. This agrees with the proposed
521 multi-step activation of endothelium in which binding results in a high local concentration of soluble
522 erythrocytic and parasitic factors [20].
523
524 A multiplex assay was used to detect 41 cytokines in the co-culture supernatant. HBMEC produce low
525 levels of cytokines in their basal state, and this is not much increased after co-culture with IE, with a
526 relatively low FC comparing IE to RBC co-culture (Supplementary Table 7). The multiplex was not
527 performed with all the isolates nor SBP1-KO, and only with one experiment, thus, the results are only an
528 indication of the effects of IE co-culture. Stimulation with TNF, as positive control, did increase the
529 concentrations of multiple cytokines, including IL-6, IL-8, IP-10 and MCP-1, also reported in other studies
530 [23,55,56]. Indeed, Zuniga et al[23] noted they observed transcriptionally similar but translationally different levels
531 of cytokines between their treatment groups even when total protein synthesis levels were similar,
532 suggesting a role for post-translational regulation in HBMEC after incubation with IE.
533
534 Whether the patient-derived isolates affect HBMEC barrier integrity was determined by TEER, with cell
535 index as measure of integrity. In all experiments, the cell index was increased after adding IE, but to a
536 similar level as RBC, likely to be due to the layer of RBC on top of the HBMEC affecting conductivity
537 (Supplementary Figure 4A and B). None of the isolates decreased the HBMEC barrier function, even after
538 24 hours (Supplementary Figure 4B). This contrasts with other studies where the addition of IE decreased
539 the barrier integrity [23,55] and is likely related to their use of schizont-stage IE or IE lysates, while trophozoite-
540 stage IE were used in our experiments. After 24 hours, parasites seemed to be in a resting stage and were
541 not progressing to schizont stage, therefore not releasing parasite factors, previously identified as the reason
542 for the decrease in barrier function [23,55,57].
543
544 It has been reported that IE affect the endothelial responses to thrombin [23,55], which reduces barrier function
545 rapidly and quickly recovers. The presence of RBC or IE affected the response of HBMEC to thrombin
546 with a reduced maximum response and AUC, compared to medium (Supplementary Figures 4E and F).
547 There were no significant differences between RBC or IE, but the non-binding lab isolates SBP1-KO, at
548 the three different parasitemias, was significantly different to the effect of 30% IE (Supplementary Figure
549 4D, E, and F), indicating that receptor binding may be required to reduce the effect of thrombin. In contrast,
550 Avril et al showed that schizont IE, but not trophozoite IE, prolonged thrombin-induced barrier disruption,
551 compared to RBC [55]. However, thrombin was added 2 – 3 hours after adding IE or RBC and not compared
552 to the effect of thrombin in medium. Thrombin decreases endothelial barrier function by cleavage of

553 Protease Activated Receptor 1 (PAR1) and involves the thrombomodulin /activated protein C system in
554 which the balance of thrombin and activated protein C determines PAR1-dependent barrier disruptive or
555 protective action, respectively [14,58]. The reduced effect of thrombin indicates a shift towards more activated
556 protein C, which was not investigated in this study. However, binding of IE to HBMEC induces receptor
557 shedding and this could change the level of thrombomodulin and endothelial protein C receptor, the
558 receptors for thrombin and protein C, respectively [57,59], affecting PAR1 cleavage. The TEER data show that
559 specific binding of IE to HBMEC do affect certain endothelial responses, not captured in the RNA
560 transcription data.
561
562 One limitation of this study was the use of a co-culture model that simplified the complex microvascular
563 system down to static interaction between IE and HBMEC. Nonetheless, this model allowed for the study
564 of the HBMEC transcriptional response to patient-derived parasites and to assess if these responses were
565 dependent on IE cytoadhesion or clinical syndrome. The ratio of 110 IE/HBMEC in our experiments is
566 similar to the range employed in other studies [23,55], which was calculated in Zuniga et al to be equivalent to
567 approximately two layers of IE on top of the HBMEC. We tested whether the Fluidigm panel would reflect
568 endothelial gene expression changes by exposing HBMEC overnight to IL-1beta and TNF and comparing
569 the gene expression with a media control (Supplementary Table 2). We observed massive upregulation in
570 HBMEC expression of several genes, including *CXCL3*, *ICAM1*, *PTGS2*, *SELE*, and *VCAM1*, after
571 incubation with both stimuli, confirming that our model was able to determine regulation of specific genes.
572 Furthermore, there was significant reduction in relative gene expression after withdrawal of TNF from
573 HBMEC (Supplementary Figure 1). Overall, these findings suggest that the changes in relative gene
574 expression observed in HBMEC exposed to both binding and non-binding parasites are due to the impact
575 of IE.
576
577 During early stages of sequestration, we observed effects on endothelium that are both dependent and
578 independent of *Pf*EMP1. These effects were relatively small except for several genes, including *CYP1A1*,
579 *KLF4*, and *PTGS2*. These genes may represent early endothelial protective responses that act through
580 vascular regulation and modulation of thrombomodulin. There was no difference in gene regulation in
581 HBMEC based on the origin of the isolate nor the parasite binding capacities. Overall, interaction of IE and
582 endothelial cells in early stages of sequestration does induce some endothelial responses, including some
583 that are independent of PfEMP1, and this is the first investigation to our knowledge to study how non-
584 *Pf*EMP1 expressing IE affect endothelial transcriptional responses. Understanding the different
585 mechanisms of crosstalk between *P. falciparum* infected erythrocytes and host endothelium may help us to

586 develop interventions that support patients with severe malaria while effective anti-parasite drugs clear the
587 infection.

588

589 **Acknowledgements:** We thank the members of staff in the NGS facility at the Bioscience Core Labs in
590 KAUST for the training and use of the Fluidigm Biomark HD system. This work was supported by
591 Competitive Research Grant (CRG) to AP and AGC (Grant number: CRG6-3392.02) by the Office of
592 Sponsored Research (OSR) at the King Abdullah University of Science and Technology (KAUST). The
593 funder had no role in study design, data collection, or preparation of the manuscript.

594

595 **Author Contributions:** Study conceptualisation: AGC; funding acquisition and administration: AGC, AP;
596 study supervision: AGC, AP, JS; study investigation: CA, JS, GC; formal analysis: CA, JS; writing –
597 original draft: CA, JS; writing – review and editing: CA, JS, AGC, AP. CA and JS determined CA would
598 be listed first as they are an early career scientist and JS is already an established researcher.

599 **References**

600 1 World Malaria Report 2023. Geneva: World Health Organization; 2023. Licence: CC BY-NC-SA 3.0 IGO. (2023).
601 2 Phillips, M. A. *et al.* Malaria. *Nat Rev Dis Primers* **3**, 17050, doi:10.1038/nrdp.2017.50 (2017).
602 3 Kojom Foko, L. P., Kumar, A., Hawadak, J. & Singh, V. Plasmodium cynomolgi in humans: current knowledge and
603 future directions of an emerging zoonotic malaria parasite. *Infection* **51**, 623-640, doi:10.1007/s15010-022-01952-2
604 (2023).
605 4 de Oliveira, T. C. *et al.* Plasmodium simium: Population Genomics Reveals the Origin of a Reverse Zoonosis. *J Infect*
606 *Dis* **224**, 1950-1961, doi:10.1093/infdis/jiab214 (2021).
607 5 Song, X. *et al.* Cerebral malaria induced by plasmodium falciparum: clinical features, pathogenesis, diagnosis, and
608 treatment. *Front Cell Infect Microbiol* **12**, 939532, doi:10.3389/fcimb.2022.939532 (2022).
609 6 Seydel, K. B. *et al.* Brain swelling and death in children with cerebral malaria. *N Engl J Med* **372**, 1126-1137,
610 doi:10.1056/NEJMoa1400116 (2015).
611 7 Mohanty, S. *et al.* Magnetic Resonance Imaging of Cerebral Malaria Patients Reveals Distinct Pathogenetic Processes
612 in Different Parts of the Brain. *mSphere* **2**, doi:10.1128/mSphere.00193-17 (2017).
613 8 Storm, J. & Craig, A. G. Pathogenesis of cerebral malaria--inflammation and cytoadherence. *Front Cell Infect*
614 *Microbiol* **4**, 100, doi:10.3389/fcimb.2014.00100 (2014).
615 9 Ramachandran, A. & Sharma, A. Dissecting the mechanisms of pathogenesis in cerebral malaria. *PLoS Pathog* **18**,
616 e1010919, doi:10.1371/journal.ppat.1010919 (2022).
617 10 Pasternak, N. D. & Dzikowski, R. PfEMP1: an antigen that plays a key role in the pathogenicity and immune evasion
618 of the malaria parasite Plasmodium falciparum. *Int J Biochem Cell Biol* **41**, 1463-1466,
619 doi:10.1016/j.biocel.2008.12.012 (2009).
620 11 Smith, J. D. The role of PfEMP1 adhesion domain classification in Plasmodium falciparum pathogenesis research. *Mol*
621 *Biochem Parasitol* **195**, 82-87, doi:10.1016/j.molbiopara.2014.07.006 (2014).
622 12 Albrecht-Schgoer, K., Lackner, P., Schmutzhard, E. & Baier, G. Cerebral Malaria: Current Clinical and Immunological
623 Aspects. *Front Immunol* **13**, 863568, doi:10.3389/fimmu.2022.863568 (2022).
624 13 Kraemer, S. M. & Smith, J. D. A family affair: var genes, PfEMP1 binding, and malaria disease. *Curr Opin Microbiol*
625 **9**, 374-380, doi:10.1016/j.mib.2006.06.006 (2006).
626 14 Bernabeu, M. & Smith, J. D. EPCR and Malaria Severity: The Center of a Perfect Storm. *Trends Parasitol* **33**, 295-
627 308, doi:10.1016/j.pt.2016.11.004 (2017).
628 15 Kessler, A. *et al.* Linking EPCR-Binding PfEMP1 to Brain Swelling in Pediatric Cerebral Malaria. *Cell Host Microbe*
629 **22**, 601-614 e605, doi:10.1016/j.chom.2017.09.009 (2017).
630 16 Turner, L. *et al.* Severe malaria is associated with parasite binding to endothelial protein C receptor. *Nature* **498**, 502-
631 505, doi:10.1038/nature12216 (2013).
632 17 Moxon, C. A., Gibbins, M. P., McGuinness, D., Milner, D. A., Jr. & Marti, M. New Insights into Malaria Pathogenesis.
633 *Annu Rev Pathol* **15**, 315-343, doi:10.1146/annurev-pathmechdis-012419-032640 (2020).

18 Lennartz, F. *et al.* Structure-Guided Identification of a Family of Dual Receptor-Binding PfEMP1 that Is Associated with Cerebral Malaria. *Cell Host Microbe* **21**, 403-414, doi:10.1016/j.chom.2017.02.009 (2017).
19 Avril, M., Bernabeu, M., Benjamin, M., Brazier, A. J. & Smith, J. D. Interaction between Endothelial Protein C Receptor and Intercellular Adhesion Molecule 1 to Mediate Binding of Plasmodium falciparum-Infected Erythrocytes to Endothelial Cells. *mBio* **7**, doi:10.1128/mBio.00615-16 (2016).
20 Gallego-Delgado, J. & Rodriguez, A. Rupture and Release: A Role for Soluble Erythrocyte Content in the Pathology of Cerebral Malaria. *Trends Parasitol* **33**, 832-835, doi:10.1016/j.pt.2017.06.005 (2017).
21 Adams, Y. *et al.* Plasmodium falciparum erythrocyte membrane protein 1 variants induce cell swelling and disrupt the blood-brain barrier in cerebral malaria. *J Exp Med* **218**, doi:10.1084/jem.20201266 (2021).
22 Bernabeu, M. *et al.* Binding Heterogeneity of Plasmodium falciparum to Engineered 3D Brain Microvessels Is Mediated by EPCR and ICAM-1. *mBio* **10**, doi:10.1128/mBio.00420-19 (2019).
23 Zuniga, M. *et al.* Plasmodium falciparum and TNF-alpha Differentially Regulate Inflammatory and Barrier Integrity Pathways in Human Brain Endothelial Cells. *mBio* **13**, e0174622, doi:10.1128/mbio.01746-22 (2022).
24 Azasi, Y. *et al.* Infected erythrocytes expressing DC13 PfEMP1 differ from recombinant proteins in EPCR-binding function. *Proc Natl Acad Sci U S A* **115**, 1063-1068, doi:10.1073/pnas.1712879115 (2018).
25 Othman, B. *et al.* Different PfEMP1-expressing Plasmodium falciparum variants induce divergent endothelial transcriptional responses during co-culture. *PLoS One* **18**, e0295053, doi:10.1371/journal.pone.0295053 (2023).
26 Storm, J. *et al.* Cerebral malaria is associated with differential cytoadherence to brain endothelial cells. *EMBO Mol Med* **11**, doi:10.15252/emmm.201809164 (2019).
27 Maier, A. G. *et al.* Skeleton-binding protein 1 functions at the parasitophorous vacuole membrane to traffic PfEMP1 to the Plasmodium falciparum-infected erythrocyte surface. *Blood* **109**, 1289-1297, doi:10.1182/blood-2006-08-043364 (2007).
28 Livak, K. J. & Schmittgen, T. D. Analysis of relative gene expression data using real-time quantitative PCR and the 2(-Delta Delta C(T)) Method. *Methods* **25**, 402-408, doi:10.1006/meth.2001.1262 (2001).
29 Madkhali, A. M. *et al.* An analysis of the binding characteristics of a panel of recently selected ICAM-1 binding Plasmodium falciparum patient isolates. *PLoS One* **9**, e111518, doi:10.1371/journal.pone.0111518 (2014).
30 Howard, C., Joof, F., Hu, R., Smith, J. D. & Zheng, Y. Probing cerebral malaria inflammation in 3D human brain microvessels. *Cell Rep* **42**, 113253, doi:10.1016/j.celrep.2023.113253 (2023).
31 Karsan, A., Yee, E., Kaushansky, K. & Harlan, J. M. Cloning of human Bcl-2 homologue: inflammatory cytokines induce human A1 in cultured endothelial cells. *Blood* **87**, 3089-3096 (1996).
32 Peters, J. M., Fowler, E. V., Krause, D. R., Cheng, Q. & Gatton, M. L. Differential changes in Plasmodium falciparum var transcription during adaptation to culture. *J Infect Dis* **195**, 748-755, doi:10.1086/511436 (2007).
33 Mkumbaye, S. I. *et al.* Cellulose filtration of blood from malaria patients for improving ex vivo growth of Plasmodium falciparum parasites. *Malar J* **16**, 69, doi:10.1186/s12936-017-1714-2 (2017).
34 Cooke, B. M. *et al.* A Maurer's cleft-associated protein is essential for expression of the major malaria virulence antigen on the surface of infected red blood cells. *J Cell Biol* **172**, 899-908, doi:10.1083/jcb.200509122 (2006).
35 Hadjilaou, A., Brandi, J., Riehn, M., Friese, M. A. & Jacobs, T. Pathogenetic mechanisms and treatment targets in cerebral malaria. *Nat Rev Neurol* **19**, 688-709, doi:10.1038/s41582-023-00881-4 (2023).
36 Moxon, C. A. *et al.* Parasite histones are toxic to brain endothelium and link blood barrier breakdown and thrombosis in cerebral malaria. *Blood Adv* **4**, 2851-2864, doi:10.1182/bloodadvances.2019001258 (2020).
37 Bachmann, A. *et al.* Highly co-ordinated var gene expression and switching in clinical Plasmodium falciparum isolates from non-immune malaria patients. *Cell Microbiol* **13**, 1397-1409, doi:10.1111/j.1462-5822.2011.01629.x (2011).
38 Lee, W. C., Russell, B. & Renia, L. Sticking for a Cause: The Falciparum Malaria Parasites Cytoadherence Paradigm. *Front Immunol* **10**, 1444, doi:10.3389/fimmu.2019.01444 (2019).
39 Chan, J. A. *et al.* A single point in protein trafficking by Plasmodium falciparum determines the expression of major antigens on the surface of infected erythrocytes targeted by human antibodies. *Cell Mol Life Sci* **73**, 4141-4158, doi:10.1007/s00018-016-2267-1 (2016).
40 Possemiers, H. *et al.* Skeleton binding protein-1-mediated parasite sequestration inhibits spontaneous resolution of malaria-associated acute respiratory distress syndrome. *PLoS Pathog* **17**, e1010114, doi:10.1371/journal.ppat.1010114 (2021).
41 Watson, E. C., Grant, Z. L. & Coultas, L. Endothelial cell apoptosis in angiogenesis and vessel regression. *Cell Mol Life Sci* **74**, 4387-4403, doi:10.1007/s00018-017-2577-y (2017).
42 Vogler, M. BCL2A1: the underdog in the BCL2 family. *Cell Death Differ* **19**, 67-74, doi:10.1038/cdd.2011.158 (2012).
43 Noble, K. E., Wickremasinghe, R. G., DeCornet, C., Panayiotidis, P. & Yong, K. L. Monocytes stimulate expression of the Bcl-2 family member, A1, in endothelial cells and confer protection against apoptosis. *J Immunol* **162**, 1376-1383 (1999).
44 Xu, S. *et al.* The zinc finger transcription factor, KLF2, protects against COVID-19 associated endothelial dysfunction. *Signal Transduct Target Ther* **6**, 266, doi:10.1038/s41392-021-00690-5 (2021).
45 SenBanerjee, S. *et al.* KLF2 Is a novel transcriptional regulator of endothelial proinflammatory activation. *J Exp Med* **199**, 1305-1315, doi:10.1084/jem.20031132 (2004).
46 Hamik, A. *et al.* Kruppel-like factor 4 regulates endothelial inflammation. *J Biol Chem* **282**, 13769-13779, doi:10.1074/jbc.M700078200 (2007).

47 Sangwung, P. *et al.* KLF2 and KLF4 control endothelial identity and vascular integrity. *JCI Insight* **2**, e91700, doi:10.1172/jci.insight.91700 (2017).
48 Zhou, G. *et al.* Endothelial Kruppel-like factor 4 protects against atherothrombosis in mice. *J Clin Invest* **122**, 4727-4731, doi:10.1172/JCI66056 (2012).
49 Atkins, G. B. & Jain, M. K. Role of Kruppel-like transcription factors in endothelial biology. *Circ Res* **100**, 1686-1695, doi:10.1161/01.RES.0000267856.00713.0a (2007).
50 Lin, Z. *et al.* Kruppel-like factor 2 (KLF2) regulates endothelial thrombotic function. *Circ Res* **96**, e48-57, doi:10.1161/01.RES.0000159707.05637.a1 (2005).
51 Ghaleb, A. M. & Yang, V. W. Kruppel-like factor 4 (KLF4): What we currently know. *Gene* **611**, 27-37, doi:10.1016/j.gene.2017.02.025 (2017).
52 Stitham, J., Midgett, C., Martin, K. A. & Hwa, J. Prostacyclin: an inflammatory paradox. *Front Pharmacol* **2**, 24, doi:10.3389/fphar.2011.00024 (2011).
53 Dorris, S. L. & Peebles, R. S., Jr. PGI2 as a regulator of inflammatory diseases. *Mediators Inflamm* **2012**, 926968, doi:10.1155/2012/926968 (2012).
54 Ferguson, C. S. & Tyndale, R. F. Cytochrome P450 enzymes in the brain: emerging evidence of biological significance. *Trends Pharmacol Sci* **32**, 708-714, doi:10.1016/j.tips.2011.08.005 (2011).
55 Avril, M., Benjamin, M., Dols, M. M. & Smith, J. D. Interplay of Plasmodium falciparum and thrombin in brain endothelial barrier disruption. *Sci Rep* **9**, 13142, doi:10.1038/s41598-019-49530-1 (2019).
56 O'Carroll, S. J. *et al.* Pro-inflammatory TNFalpha and IL-1beta differentially regulate the inflammatory phenotype of brain microvascular endothelial cells. *J Neuroinflammation* **12**, 131, doi:10.1186/s12974-015-0346-0 (2015).
57 Storm, J., Wu, Y., Davies, J., Moxon, C. A. & Craig, A. G. Testing the effect of PAR1 inhibitors on Plasmodium falciparum-induced loss of endothelial cell barrier function. *Wellcome Open Res* **5**, 34, doi:10.12688/wellcomeopenres.15602.3 (2020).
58 Alberelli, M. A. & De Candia, E. Functional role of protease activated receptors in vascular biology. *Vascul Pharmacol* **62**, 72-81, doi:10.1016/j.vph.2014.06.001 (2014).
59 Moxon, C. A. *et al.* Persistent endothelial activation and inflammation after Plasmodium falciparum Infection in Malawian children. *J Infect Dis* **209**, 610-615, doi:10.1093/infdis/jit419 (2014).
60 Mkumbaye, S. I. *et al.* The Severity of Plasmodium falciparum Infection Is Associated with Transcript Levels of var Genes Encoding Endothelial Protein C Receptor-Binding P. falciparum Erythrocyte Membrane Protein 1. *Infect Immun* **85**, doi:10.1128/IAI.00841-16 (2017).

Results Figures and Tables

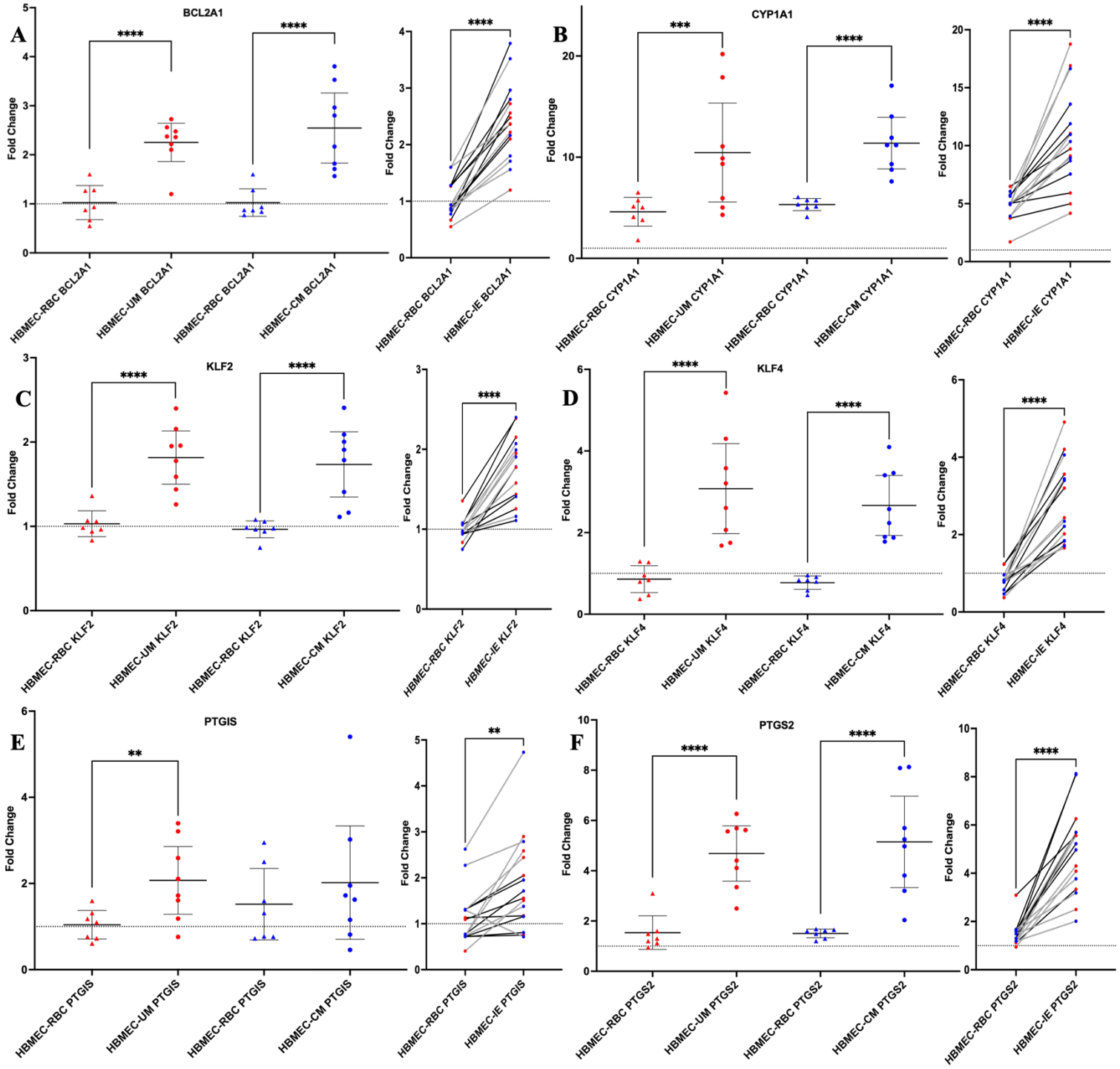

Figure 1: **IE of both UM and CM clinical isolates affect HBMEC transcriptional responses as compared to RBC**. Differential gene expression of HBMEC after 6-hour co-culture with patient-derived parasites compared to their corresponding RBCs for *BCL2A1*(A), *CYP1A1*(B), *KLF2*(C), *KLF4*(D), *PTGIS*(E), and *PTGS2*(F), calculated as relative to the corresponding 6-hour HBMEC-media control. Mean HBMEC gene expression (Fold Change) was compared in two ways for the selected genes: (left) Welch's t-test comparing HBMEC-RBC and HBMEC-IE for UM or CM isolates and (right) paired t-test comparing all RBC controls and the combined HBMEC-IE of all isolates. The Welch's t-test results shown in the graphs are from Supplementary

Figure1. Each point on the plot represents one sample FC, calculated as a mean of the technical triplicates, and the mean and 95% confidence intervals are indicated for each group. For the paired analysis, the mean FC was calculated from technical triplicates for each IE and corresponding RBC sample and are coloured red for UM isolates and blue for CM isolates. A paired t-test was performed comparing the mean FC of HBMEC-IE with the corresponding HBMEC-RBC. Lines between the groups indicate that the RBC sample on the left was the control for the corresponding isolate sample on the right. Black lines represent samples from experiment 1, and grey lines represent samples from experiment 2. Two-tailed tests were performed for both analyses, and the dotted line in the plots marks the baseline of FC=1. Significance is depicted by the P-value: *,0.01-0.05; **, 0.001-0.01; ***, 0.0001-0.001; ****, <0.0001.

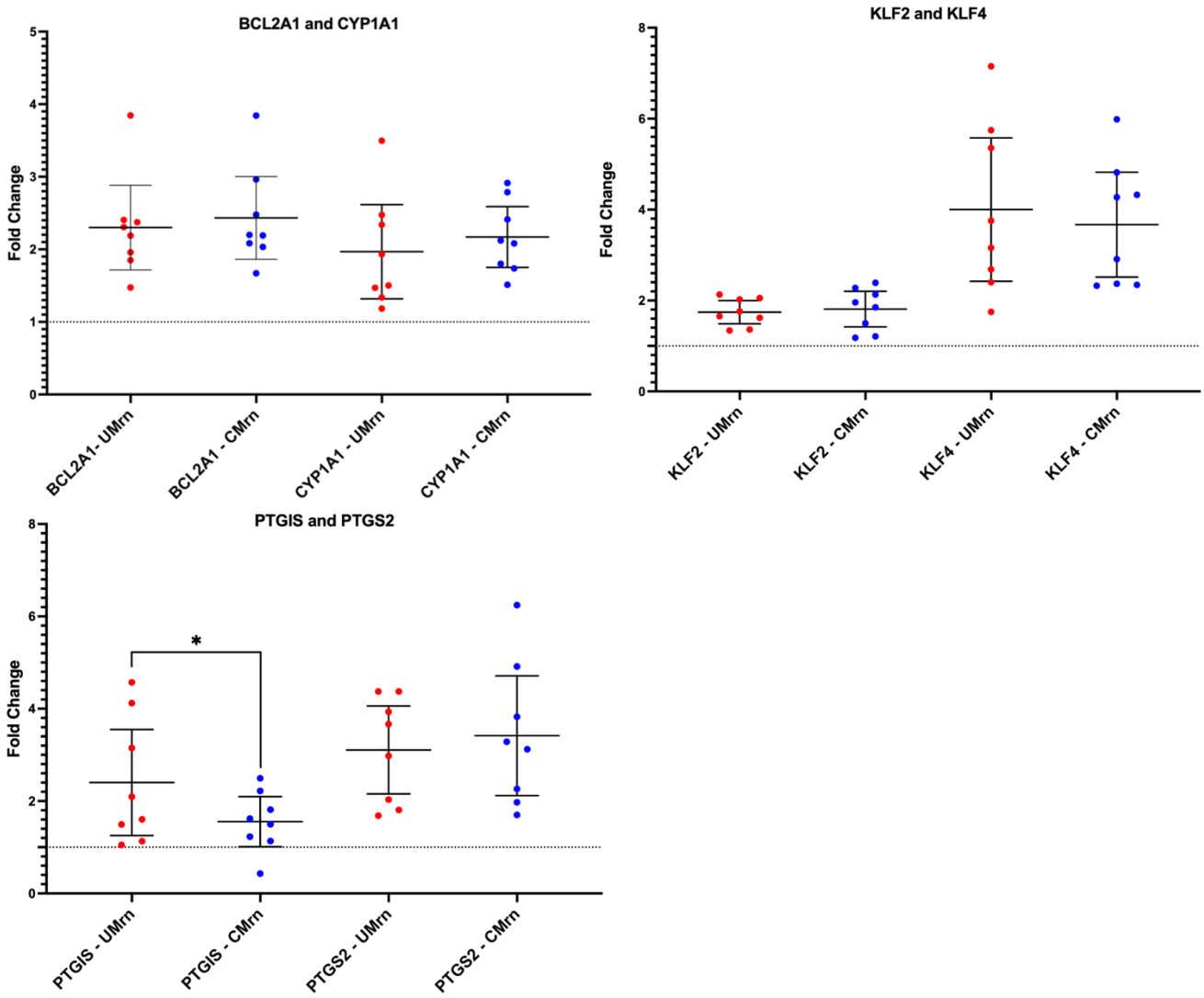

Figure 2: **When normalized to HBMEC-RBC controls, isolates within clinical categories do not induce differential responses in HBMEC.** To determine the effect of the parasites, HBMEC relative gene expression when exposed to UM and CM patient-derived isolates was calculated relative to HBMEC-RBC expression, using GAPDH as the endogenous control and the 6-hour HBMEC-RBC as the normalization sample reference. Each point represents one experimental sample (mean of triplicates), and the mean FC and 95% confidence intervals for each gene was calculated using both biological replicates (n= 8). RBC normalized HBMEC-UM is represented as "UMrn", and RBC-normalized HBMEC-CM is represented as "CMrn". Significance between the two clinical categories was determined by two-tailed unpaired T-tests with P-value summary defined =*,0.01-0.05. The dotted line marks the baseline of FC=1 (red = UM isolates; blue = CM isolates).

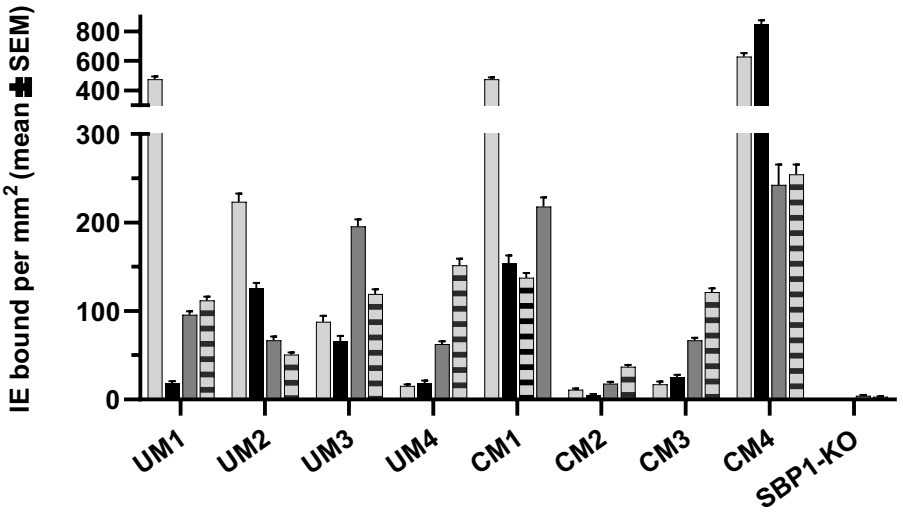

753

754 ***Figure 3:*** **Binding of patient-derived isolates to HBMEC under flow conditions.** Binding of IE to TNF-stimulated HBMEC or
755 HDMEC was determined using microfluidics. Shown is the mean ± SEM IE/mm^2 EC cell surface of 15 fields counted by
756 microscopy. The level of binding for the UM and CM-derived isolates shortly after isolation from the patients is depicted in light
757 grey (HDMEC) and in black (HBMEC). After certain days in culture (DIC) binding of HBMEC is depicted in dark grey (experiment
758 2) and light grey with horizontal bars (experiment 1). UM1: 30 and 64 DIC, UM2: 32 and 50 DIC, UM3: 40 and 44 DIC, UM4: 25
759 and 38 DIC, CM1: 31 and 36 DIC, CM2: 32 and 46 DIC, CM3: 50 and 66 DIC, CM4: 42 and 46 DIC. SBP1-KO does not bind to
760 HBMEC.

761

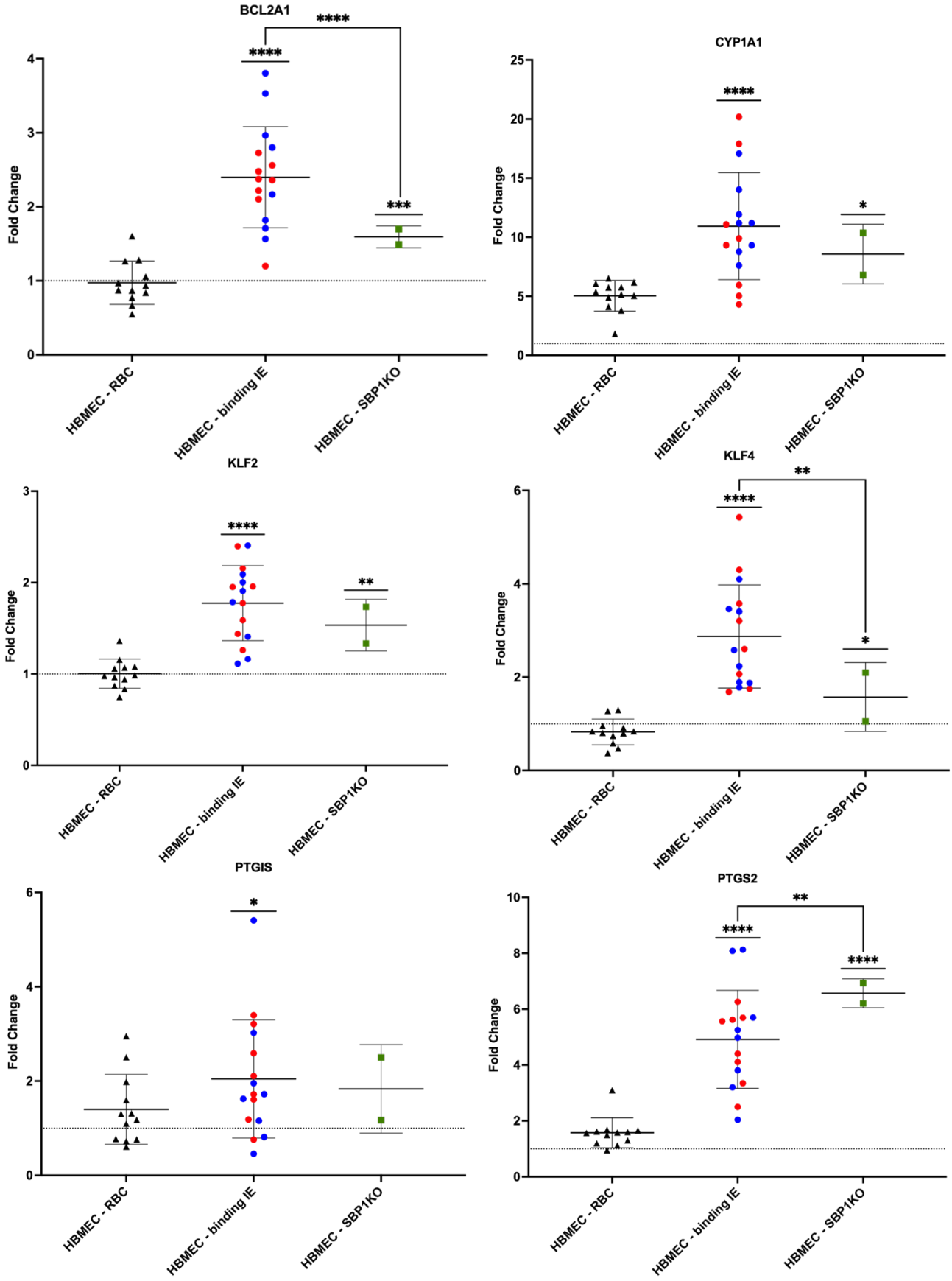
BCL2A1
****
****
***
Fold Change
HBMEC - RBC
HBMEC - binding IE
HBMEC - SBP1KO
CYP1A1
****
*
KLF2
****
**
KLF4
**
****
*
PTGIS
*
PTGS2
**
****
****

762

763 ***Figure 4:*** **Observed differential effects on HBMEC transcriptional response is not due to binding to HBMEC.** Relative gene
764 expression of HBMEC exposed to patient-derived parasites that bind to HBMEC and the non-binding SBP1-KO parasites for 6
765 hours compared to corresponding RBCs for select genes. HBMEC-RBC samples for both binding and non-binding IE were
766 combined for plotting. Each point on the plot represents one sample FC, calculated as a mean of the technical triplicates, and the
767 mean and 95% confidence intervals are indicated for each group. FC was calculated using GAPDH as an endogenous control and
768 relative to the 6-hour HBMEC-media normalization control (baseline is FC =1). Welch's t-tests were used to compare HBMEC-
769 RBC and HBMEC-IE for each of the parasite groups, and the mean FC ± SEM for each gene was calculated using the two biological
770 replicates for 4 UM and 4 CM isolates and their corresponding RBC (HBMEC-RBC (binding) n = 10, HBMEC-binding IE n =16,
771 HBMEC-RBC(SBP1KO) and HBMEC-SBP1KO (n =2). The results of the Welch's t-tests comparing the HBMEC-IE groups with
772 corresponding HBMEC-RBC are summarized in Supplementary Table 3. Sample grouping is represented by symbol, with triangles
773 for HBMEC-RBC, circles for HBMEC-binding IE, and squares for HBMEC-SBP1KO. For binding IE, the red data points represent
774 UM samples, while the blue data points represent CM samples. Samples from experiments with the non-binding parasites are in
775 green. Significant relationships between HBMEC-IE groups and the corresponding HBMEC-RBC are indicated by straight bars
776 over the IE groups ($p<0.05$), and the P-value summaries are from the calculations performed in Supplementary Table 3. For
777 *BCL2A1*, *KLF4*, and *PTGS2*, the results of Welch's t-tests comparing HBMEC-binding and HBMEC-SBP1KO are indicated by the
778 bent lines connecting between these groups ($p<0.05$), and the P-value summaries are from the calculations performed in
779 Supplementary Table 4. In all plots, the dotted line marks the baseline of FC=1. P-value summary defined= *,0.01-0.05; **, 0.001-
780 0.01; ***, 0.0001-0.001; ****, <0.0001).
781
782
783
784
785
786
787
788
789
790
791
792
793
794
795
796
797
798
799
800

Supplementary Data

Supplementary Table 1: **Relative gene expression of HBMEC co-cultured with IE from patient-derived isolates or with the corresponding RBC control for each gene in the panel.** Samples were collected after a 6-hour co-culture, and relative gene expression was calculated using the ΔΔCt method using GAPDH as the endogenous control and the corresponding experimental 6-hour HBMEC-media sample as the reference sample (baseline is FC =1). The mean Fold Change (FC) and standard error of the mean (SEM) for each gene were calculated using the technical triplicates of the two biological replicates (UM = uncomplicated malaria patient-derived isolates, CM = cerebral malaria patient-derived isolates, n = sample size). Rows shaded in dark grey have FC>1.5 for one of the IE groups. P-value summary defined= *,0.01-0.05; **, 0.001-0.01; ***, 0.0001-0.001; ****, <0.0001.

	WELCH'S T-TEST COMPARING HBMEC-RBC (N=21) AND HBMEC-UM (N=24) RELATIVE FC				**WELCH'S T-TEST COMPARING HBMEC-RBC (N=21) AND HBMEC-CM (N=24) RELATIVE FC**			
GENE	HBMEC-RBC(UM) mean FC ± SEM	HBMEC-UM mean FC ± SEM	P value	P value summary	HBMEC-RBC(CM) mean FC ± SEM	HBMEC-CM mean FC ± SEM	P value	P value summary
ACTB	1.01 ± 0.026	1.12 ± 0.053	0.0039	**	0.94 ± 0.02	1.23 ± 0.047	<0.0001	****
ACTG1	1.03 ± 0.028	1.25 ± 0.033	<0.0001	****	1.01 ± 0.021	1.29 ± 0.046	<0.0001	****
ADAM10	1.01 ± 0.016	1.16 ± 0.031	0.0002	***	1 ± 0.021	1.13 ± 0.028	0.0012	**
ADAM17	0.92 ± 0.04	1.14 ± 0.025	<0.0001	****	0.91 ± 0.027	1.1 ± 0.04	0.0002	***
ANGTP2	1.05 ± 0.037	0.9 ± 0.025	0.0014	**	1.09 ± 0.021	0.96 ± 0.043	0.0075	**
ANK1	0.84 ± 0.049	0.99 ± 0.087	0.1365	ns	0.91 ± 0.086	1.22 ± 0.17	0.1132	ns
BAX	0.97 ± 0.028	0.98 ± 0.031	0.8577	ns	0.97 ± 0.022	1 ± 0.024	0.2942	ns
BCL2A1	1.03 ± 0.078	2.25 ± 0.093	<0.0001	****	1.03 ± 0.064	2.55 ± 0.171	<0.0001	****
CASP3	1.05 ± 0.041	1.07 ± 0.064	0.7753	ns	1.01 ± 0.03	0.98 ± 0.041	0.6767	ns
CCL14	0.96 ± 0.038	0.67 ± 0.035	<0.0001	****	1 ± 0.039	0.78 ± 0.031	0.0001	***
CDH5	0.99 ± 0.022	1.02 ± 0.022	0.3607	ns	0.96 ± 0.024	1 ± 0.013	0.1881	ns
CXCL3	0.79 ± 0.106	1.82 ± 0.26	0.0009	***	0.86 ± 0.097	1.72 ± 0.184	0.0002	***
CYP1A1	4.6 ± 0.374	10.46 ± 1.388	0.0004	***	5.32 ± 0.299	11.39 ± 0.838	<0.0001	****
DUSP5	0.96 ± 0.032	1.52 ± 0.048	<0.0001	****	0.91 ± 0.045	1.44 ± 0.069	<0.0001	****
EEF1A1	1.01 ± 0.056	1.21 ± 0.058	0.0195	*	0.97 ± 0.04	1.22 ± 0.06	0.0012	**
FAS	0.96 ± 0.058	0.96 ± 0.072	0.9836	ns	1.02 ± 0.057	0.94 ± 0.048	0.302	ns
HES1	1.05 ± 0.043	1.32 ± 0.075	0.004	**	1.02 ± 0.045	1.28 ± 0.088	0.0135	*
HEY1	0.81 ± 0.055	0.84 ± 0.054	0.7524	ns	0.73 ± 0.045	0.74 ± 0.048	0.8462	ns
HEY2	1.38 ± 0.123	1.24 ± 0.118	0.4226	ns	1.43 ± 0.116	1.38 ± 0.138	0.7798	ns
ICAM1	1 ± 0.109	1.39 ± 0.144	0.0358	*	0.97 ± 0.109	1.41 ± 0.116	0.0088	**
IL1A	1.21 ± 0.085	1.92 ± 0.106	<0.0001	****	1.27 ± 0.084	1.99 ± 0.112	<0.0001	****
IL6	1.16 ± 0.062	1.39 ± 0.053	0.0079	**	1.01 ± 0.033	1.59 ± 0.103	<0.0001	****
KLF10	1.04 ± 0.031	1.17 ± 0.071	0.0986	ns	0.97 ± 0.037	1.02 ± 0.057	0.4834	ns
KLF2	1.03 ± 0.039	1.82 ± 0.079	<0.0001	****	0.96 ± 0.029	1.73 ± 0.096	<0.0001	****
KLF3	0.93 ± 0.065	1.02 ± 0.033	0.2563	ns	0.89 ± 0.039	1 ± 0.031	0.0452	*
KLF4	0.86 ± 0.089	3.08 ± 0.339	<0.0001	****	0.77 ± 0.061	2.67 ± 0.208	<0.0001	****
LAMC2	1 ± 0.034	1.14 ± 0.034	0.0039	**	0.98 ± 0.038	1.2 ± 0.051	0.0016	**
MIB1	1.09 ± 0.034	1.31 ± 0.047	0.0005	***	0.98 ± 0.039	1.26 ± 0.046	<0.0001	****
NFKB1	1 ± 0.039	1.1 ± 0.059	0.1724	ns	0.93 ± 0.031	0.94 ± 0.038	0.8053	ns
NFKBIA	0.81 ± 0.057	0.9 ± 0.053	0.2358	ns	0.82 ± 0.057	0.87 ± 0.045	0.4546	ns

NOTCH2	1.04 ± 0.104	1.16 ± 0.105	0.4248	ns	1.03 ± 0.109	1.48 ± 0.197	0.054	ns
OCLN	0.97 ± 0.081	0.87 ± 0.072	0.3534	ns	0.9 ± 0.061	1.02 ± 0.047	0.1321	ns
PAPLN	1.1 ± 0.082	1.53 ± 0.095	0.0013	**	1.07 ± 0.073	1.47 ± 0.127	0.01	**
PECAM1	0.92 ± 0.027	1.08 ± 0.033	0.0006	***	0.92 ± 0.019	1.07 ± 0.024	<0.0001	****
PLA2G4A	1.23 ± 0.071	1.49 ± 0.095	0.0336	*	1.04 ± 0.06	1.3 ± 0.078	0.0113	*
PLXNA4	1.44 ± 0.318	1.37 ± 0.308	0.8739	ns	1.24 ± 0.314	1.35 ± 0.285	0.8057	ns
PROCR	1.03 ± 0.024	1.22 ± 0.04	0.0002	***	0.99 ± 0.029	1.25 ± 0.052	<0.0001	****
PTGIS	1.04 ± 0.122	2.07 ± 0.284	0.0022	**	1.52 ± 0.255	2.02 ± 0.391	0.2894	ns
PTGS2	1.54 ± 0.153	4.69 ± 0.275	<0.0001	****	1.51 ± 0.048	5.15 ± 0.431	<0.0001	****
S100A10	0.92 ± 0.026	1 ± 0.029	0.0526	ns	0.94 ± 0.019	1.04 ± 0.019	0.0007	***
SELE	0.72 ± 0.111	0.78 ± 0.111	0.7099	ns	0.87 ± 0.125	1.46 ± 0.135	0.0023	**
SMAD6	1.4 ± 0.099	1.66 ± 0.125	0.1028	ns	1.14 ± 0.097	1.82 ± 0.178	0.0019	**
TGFB1	1 ± 0.033	1.17 ± 0.045	0.0039	**	0.94 ± 0.027	1.11 ± 0.039	0.0013	**
TJP1	0.99 ± 0.031	0.93 ± 0.032	0.1611	ns	0.9 ± 0.031	0.93 ± 0.03	0.4792	ns
TNFRSF12A	1.31 ± 0.084	1.3 ± 0.147	0.9386	ns	1.14 ± 0.105	1.08 ± 0.089	0.626	ns
TSPAN13	0.96 ± 0.052	1.1 ± 0.052	0.0645	ns	0.93 ± 0.049	1.06 ± 0.04	0.0457	*
TUBB	1.02 ± 0.02	1.02 ± 0.026	0.9383	ns	0.98 ± 0.016	1.05 ± 0.02	0.0115	*
TXNIP	1.47 ± 0.165	2.63 ± 0.485	0.0311	*	0.98 ± 0.054	2.9 ± 0.64	0.0064	**
VCAM1	0.83 ± 0.083	1.78 ± 0.121	<0.0001	****	0.85 ± 0.087	2.06 ± 0.252	<0.0001	****

Supplementary Table 2: **Assessment of endothelial responses and Fluidigm panel through relative gene expression of HBMEC after overnight incubation with inflammatory cytokines**. HBMEC were incubated overnight with either EGM2min media, 1 ng/mL IL-1beta, or 10 ng/mL TNF. The samples were collected directly after stimulation, and the relative gene expression was determined for several genes.. FCs were calculated using GAPDH as an endogenous control as relative to the HBMEC-overnight media normalization control (baseline is FC=1). The mean FC for each gene was calculated from technical triplicates from one experiment (n=3).

GENE	HBMEC-OVN MEDIA RELATIVE FC	HBMEC OVN IL-1B RELATIVE FC	HBMEC-OVN TNF RELATIVE FC
BCLA2A1	1	4.7	6.0
CXCL3	1	1305	862
CYP1A1	1	1.1	0.6
ICAM1	1	16	25
IL1A	1	40	30
IL1B	1	60	5.4
KLF2	1	1.1	1.0
KLF4	1	3.1	2.9
PTGIS	1	0.8	1.2
PTGS2	1	30	16
SELE	1	72	52
VCAM1	1	548	873

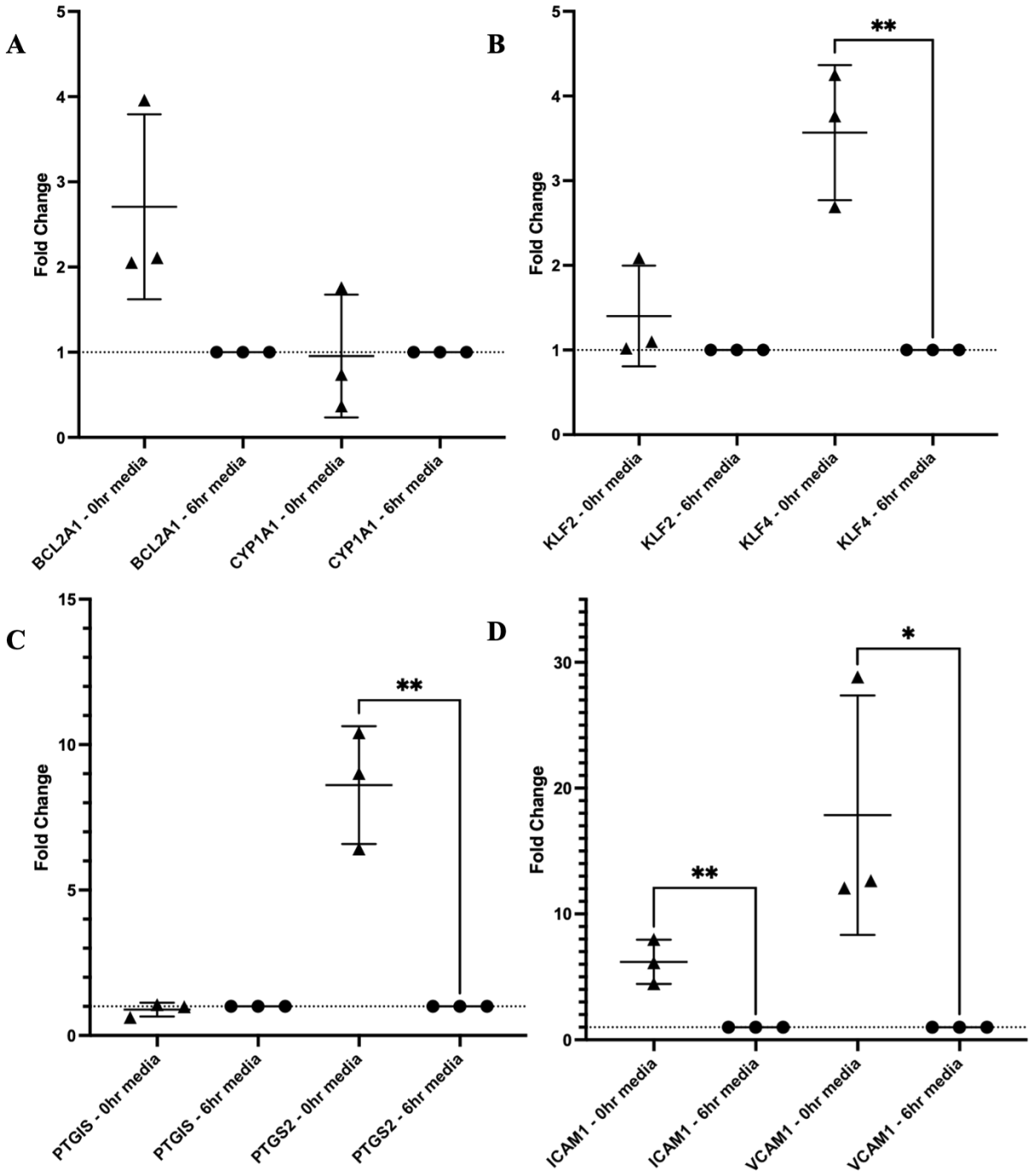

Supplementary Figure 1: **Representative relative gene expression of HBMEC after withdrawal of TNF stimulation.** In the co-culture model, HBMEC are stimulated overnight with 10 ng/mL of TNF to stimulate the cells. The next morning, the supernatant containing TNF was removed and replaced with EGM2min media for two hours before co-culture experiments commenced. HBMEC-media samples were collected at 0hr and 6hour culture time points, corresponding to 2- and 8-hours incubation with EGM2min media and without TNF, respectively. Relative gene expression was determined for (A) *BCL2A1* and *CYP1A1*, (B) *KLF2* and *KLF4*, (C) *PTGIS* and *PTGS2*, and (D) *ICAM-1* and *VCAM1* for HBMEC-media samples for three independent, representative experiments (n=3). FCs were calculated using GAPDH as an endogenous control as relative to the HBMEC-6hour media normalization control (baseline is FC=1). Each plot point represents a mean of the technical triplicates, and the mean ± SD of the 3 experiments is shown with triangle points representing HBMEC-0hr media samples and circular points representing HBMEC-6hr media samples.

827

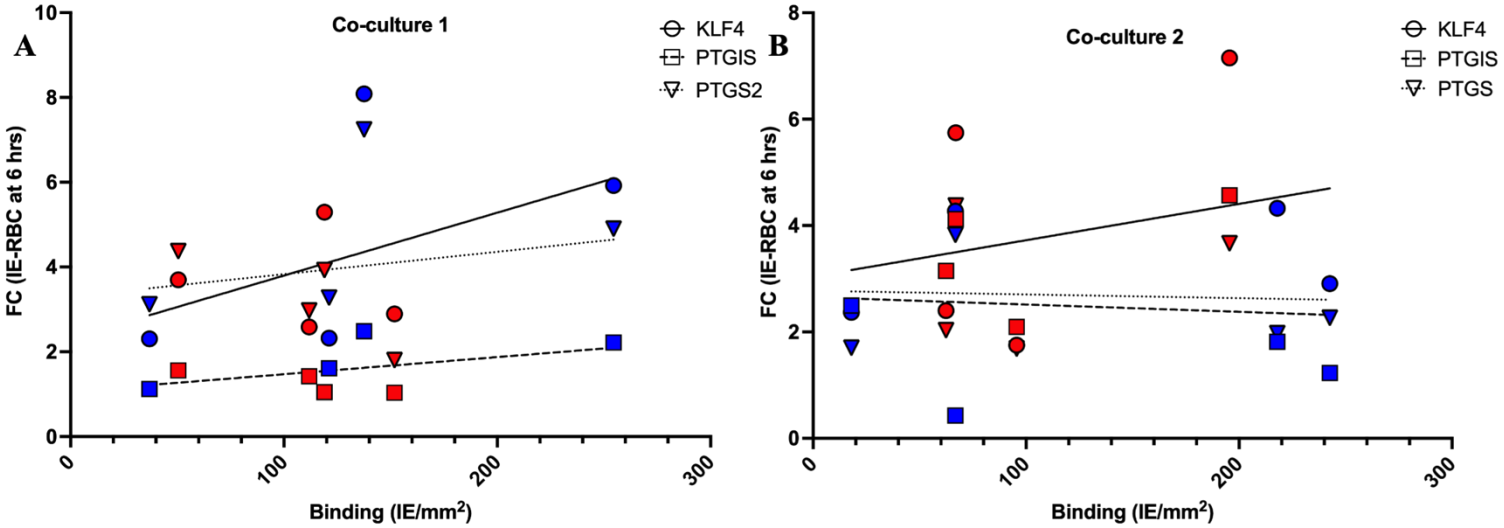

Supplementary Figure 2: **Binding capacities of patient-derived parasite isolates do not correlate with HBMEC gene expression.** The binding capacity of each isolate (IE/ mm^2) was compared to the 6-hour HBMEC mean FC relative gene expression for select genes (red = UM isolates; blue = CM isolates) after the first (A) and second (B) experiments using a linear regression. The linear regression for KLF4, PTGIS, and PTGS2 are indicated on each graph by straight, dashed, and dotted lines, respectively, and the R^2 values are reported as follows: Co-culture 1) KLF4 = 0.22, PTGIS= 0.25, PTGS2= 0.05; Co-culture 2) KLF4 = 0.10, PTGIS= 0.01, PTGS2= 0.003. Relative gene expression was calculated for HBMEC-IE using the ΔΔCt method with GAPDH as the endogenous control and the corresponding 6-hour HBMEC-RBC as the reference sample (baseline is FC=1). Each point represents the mean FC for each HBMEC-IE sample (n=8), calculated from the technical triplicates. Pearson's correlation was performed to compare parasite binding capacity to the differential gene expression for each isolate for both experiments, and the correlation coefficient (r) values are reported as follows: Co-culture 1) KLF4 = 0.47, PTGIS= 0.50, PTGS2= 0.22; Co-culture 2) KLF4 = 0.31, PTGIS= -0.08, PTGS2= -0.05.

828

829 ***Supplementary Table 3:*** **Relative gene expression of HBMEC co-cultured with either binding IE or non-binding IE compared**
830 **to the corresponding HBMEC-RBC control for each gene in the panel.** All samples were from a 6-hour time point. Data from
831 UM and CM patient-derived parasite isolates were combined to form a group of binding parasites, while two experiments with
832 non-binding SBP1KO parasites were performed. Relative gene expression was calculated using the ΔΔCt method using GAPDH
833 as the endogenous control and the corresponding experimental 6-hour HBMEC-media sample as the reference sample (baseline is
834 FC=1). The mean Fold Change (FC) and standard error of the mean (SEM) for each gene were calculated using all experimental
835 samples and technical replicates (SBP1KO= SBP1-knockout parasites, n = sample size). Rows shaded in dark grey have FC>1.5
836 for one of the HBMEC groups. P-value summary defined= *,0.01-0.05; **, 0.001-0.01; ***, 0.0001-0.001; ****, <0.0001.

	WELCH'S T-TEST COMPARING HBMEC-RBC (N=30) AND HBMEC-BINDING (N=48) RELATIVE FC				**WELCH'S T-TEST COMPARING HBMEC-RBC (N=6) AND HBMEC-SBP1KO (N=6) RELATIVE FC**			
GENE	HBMEC-RBC mean FC ± SEM	HBMEC-binding mean FC ± SEM	P value	P value summary	HBMEC-RBC mean FC ± SEM	HBMEC-SBP1KO mean FC ± SEM	P value	P value summary
ACTB	0.97 ± 0.022	1.21 ± 0.035	<0.0001	****	0.96 ± 0.035	1.06 ± 0.02	0.0372	*
ACTG1	1.01 ± 0.021	1.27 ± 0.028	<0.0001	****	0.95 ± 0.035	0.98 ± 0.032	0.6649	ns
ADAM10	1.01 ± 0.016	1.14 ± 0.021	<0.0001	****	0.88 ± 0.044	1.03 ± 0.04	0.0299	*
ADAM17	0.93 ± 0.03	1.12 ± 0.023	<0.0001	****	0.87 ± 0.036	1.05 ± 0.033	0.0045	**
ANGTP2	1.06 ± 0.027	0.93 ± 0.025	0.0007	***	1.01 1.01 ± 0.025	0.94 ± 0.04	0.1918	ns
ANK1	0.88 ± 0.065	1.1 ± 0.096	0.0535	ns	0.83 ± 0.184	0.83 ± 0.098	0.9934	ns

BAX	0.98 ± 0.02	0.99 ± 0.019	0.7438	ns	0.96 ± 0.05	0.81 ± 0.039	0.0424	*
BCL2A1	0.97 ± 0.057	2.4 ± 0.099	<0.0001	****	1.01 ± 0.078	1.59 ± 0.058	0.0002	***
CASP3	1.02 ± 0.033	1.03 ± 0.038	0.8538	ns	0.94 ± 0.056	0.87 ± 0.059	0.3719	ns
CCL14	0.96 ± 0.031	0.73 ± 0.025	<0.0001	****	0.75 ± 0.06	0.48 ± 0.022	0.0052	**
CDH5	0.96 ± 0.019	1.01 ± 0.013	0.0399	*	0.98 ± 0.023	0.88 ± 0.016	0.0075	**
CXCL3	0.8 ± 0.075	1.77 ± 0.157	<0.0001	****	2.17 ± 0.371	2.89 ± 0.551	0.3076	ns
CYP1A1	4.94 ± 0.314	10.92 ± 0.805	<0.0001	****	5.54 ± 0.604	8.57 ± 1.017	0.0329	*
DUSP5	0.9 ± 0.033	1.48 ± 0.042	<0.0001	****	1.06 ± 0.111	2.11 ± 0.138	0.0002	***
EEF1A1	0.97 ± 0.042	1.22 ± 0.041	<0.0001	****	0.89 ± 0.06	0.84 ± 0.023	0.4657	ns
FAS	1 ± 0.05	0.95 ± 0.043	0.4783	ns	0.75 ± 0.079	0.69 ± 0.062	0.6216	ns
HES1	1.01 ± 0.034	1.3 ± 0.057	<0.0001	****	0.9 ± 0.036	1.47 ± 0.056	<0.0001	****
HEY1	0.79 ± 0.046	0.79 ± 0.037	0.8966	ns	0.76 ± 0.088	0.62 ± 0.04	0.1779	ns
HEY2	1.32 ± 0.095	1.31 ± 0.09	0.9267	ns	0.91 ± 0.202	1.47 ± 0.359	0.2132	ns
ICAM1	1 ± 0.08	1.4 ± 0.091	0.0016	**	1.24 ± 0.118	1.73 ± 0.293	0.1706	ns
IL1A	1.23 ± 0.063	1.95 ± 0.076	<0.0001	****	1.5 ± 0.095	1.91 ± 0.177	0.077	ns
IL6	1.11 ± 0.048	1.49 ± 0.059	<0.0001	****	1.32 ± 0.085	1.7 ± 0.149	0.0551	ns
KLF10	0.98 ± 0.029	1.09 ± 0.046	0.048	*	1.18 ± 0.112	1.3 ± 0.108	0.4584	ns
KLF2	1 ± 0.032	1.78 ± 0.062	<0.0001	****	1.01 ± 0.073	1.53 ± 0.12	0.0056	**
KLF3	0.94 ± 0.046	1.01 ± 0.022	0.1811	ns	0.9 ± 0.042	0.7 ± 0.032	0.005	**
KLF4	0.84 ± 0.069	2.87 ± 0.199	<0.0001	****	0.77 ± 0.098	1.58 ± 0.254	0.0239	*
LAMC2	0.99 ± 0.029	1.17 ± 0.031	<0.0001	****	1.12 ± 0.093	1.24 ± 0.142	0.482	ns
MIB1	1.04 ± 0.033	1.29 ± 0.033	<0.0001	****	0.73 ± 0.052	1.16 ± 0.046	0.0001	***
NFKB1	0.98 ± 0.03	1.02 ± 0.037	0.445	ns	0.79 ± 0.062	0.7 ± 0.059	0.2969	ns
NFKBIA	0.82 ± 0.041	0.89 ± 0.034	0.2302	ns	1.16 ± 0.085	1.13 ± 0.102	0.8297	ns
NOTCH2	1.05 ± 0.089	1.32 ± 0.113	0.0702	ns	1.6 ± 0.821	2.62 ± 1.152	0.4893	ns
OCLN	0.95 ± 0.058	0.94 ± 0.044	0.9851	ns	0.88 ± 0.084	0.92 ± 0.095	0.7435	ns
PAPLN	1.04 ± 0.065	1.5 ± 0.079	<0.0001	****	0.95 ± 0.149	1 ± 0.083	0.7714	ns
PECAM1	0.91 ± 0.02	1.07 ± 0.02	<0.0001	****	0.96 ± 0.034	0.91 ± 0.032	0.2936	ns
PLA2G4A	1.15 ± 0.057	1.4 ± 0.062	0.0046	**	1.31 ± 0.224	1.51 ± 0.173	0.4987	ns
PLXNA4	1.32 ± 0.225	1.36 ± 0.207	0.9008	ns	1.01 ± 0.267	0.58 ± 0.068	0.1718	ns
PROCR	0.99 ± 0.022	1.24 ± 0.033	<0.0001	****	0.89 ± 0.037	0.92 ± 0.033	0.5743	ns
PTGIS	1.35 ± 0.188	2.05 ± 0.239	0.0252	*	1.64 ± 0.367	1.84 ± 0.442	0.7465	ns
PTGS2	1.57 ± 0.107	4.92 ± 0.255	<0.0001	****	1.58 ± 0.144	6.57 ± 0.422	<0.0001	****
S100A10	0.93 ± 0.02	1.02 ± 0.017	0.001	**	0.93 ± 0.053	0.82 ± 0.045	0.1704	ns
SELE	0.88 ± 0.1	1.12 ± 0.1	0.0935	ns	1.45 ± 0.286	2.66 ± 0.298	0.0147	*
SMAD6	1.25 ± 0.082	1.74 ± 0.108	0.0005	***	1.74 ± 0.381	1.52 ± 0.178	0.6283	ns
TGFB1	0.97 ± 0.025	1.14 ± 0.03	<0.0001	****	0.93 ± 0.042	1.14 ± 0.065	0.0236	*
TJP1	0.94 ± 0.028	0.93 ± 0.022	0.7211	ns	0.85 ± 0.069	0.77 ± 0.048	0.3735	ns
TNFRSF12A	1.24 ± 0.087	1.19 ± 0.087	0.6808	ns	1.2 ± 0.184	0.84 ± 0.171	0.1886	ns
TSPAN13	0.93 ± 0.038	1.08 ± 0.033	0.0051	**	0.86 ± 0.044	0.84 ± 0.033	0.6971	ns
TUBB	1.01 ± 0.017	1.04 ± 0.016	0.2726	ns	0.88 ± 0.044	0.9 ± 0.036	0.8362	ns

TXNIP	1.29 ± 0.129	2.76 ± 0.397	0.0008	***	0.81 ± 0.11	0.98 ± 0.18	0.4599	ns
VCAM1	0.84 ± 0.065	1.92 ± 0.14	<0.0001	****	1.13 ± 0.067	3.84 ± 0.482	0.0023	**

Supplementary Table 4: **Comparing the relative gene expression of HBMEC co-cultured with either binding IE or non-binding IE for each gene in the panel.** Welch's T-test was performed to compare the mean FC expression of HBMEC incubated with either binding or no-binding IE. All samples were from a 6-hour time point. Data from UM and CM patient-derived parasite isolates were combined to form a group of binding parasites, while two experiments with non-binding SBP1KO parasites were performed. Relative gene expression was calculated using the ΔΔCt method using GAPDH as the endogenous control and the corresponding experimental 6-hour HBMEC-media sample as the reference sample (baseline is FC=1). The mean Fold Change (FC) and standard error of the mean (SEM) for each gene were calculated using all experimental samples and technical replicates (SBP1KO= SBP1-knockout parasites, n = sample size). Rows shaded in dark grey have FC>1.5 for one of the HBMEC groups. P-value summary defined= *,0.01-0.05; **, 0.001-0.01; ***, 0.0001-0.001; ****, <0.0001.

	WELCH'S T-TEST COMPARING HBMEC-BINDING (N=48) AND HBMEC-SBP1KO (N=6) RELATIVE FC			
GENE	HBMEC-binding mean FC ± SEM	HBMEC-SBP1KO mean FC ± SEM	P value	P value summary
ACTB	1.21 ± 0.035	1.06 ± 0.02	0.0004	***
ACTG1	1.27 ± 0.028	0.98 ± 0.032	<0.0001	****
ADAM10	1.14 ± 0.021	1.03 ± 0.04	0.0366	*
ADAM17	1.12 ± 0.023	1.05 ± 0.033	0.1025	ns
ANGTP2	0.93 ± 0.025	0.94 ± 0.04	0.7908	ns
ANK1	1.1 ± 0.096	0.83 ± 0.098	0.0647	ns
BAX	0.99 ± 0.019	0.81 ± 0.039	0.0039	**
BCL2A1	2.4 ± 0.099	1.59 ± 0.058	<0.0001	****
CASP3	1.03 ± 0.038	0.87 ± 0.059	0.0452	*
CCL14	0.73 ± 0.025	0.48 ± 0.022	<0.0001	****
CDH5	1.01 ± 0.013	0.88 ± 0.016	<0.0001	****
CXCL3	1.77 ± 0.157	2.89 ± 0.551	0.0993	ns
CYP1A1	10.92 ± 0.805	8.57 ± 1.017	0.0935	ns
DUSP5	1.48 ± 0.042	2.11 ± 0.138	0.0047	**
EEF1A1	1.22 ± 0.041	0.84 ± 0.023	<0.0001	****
FAS	0.95 ± 0.043	0.69 ± 0.062	0.0066	**
HES1	1.3 ± 0.057	1.47 ± 0.056	0.0401	*
HEY1	0.79 ± 0.037	0.62 ± 0.04	0.0062	**
HEY2	1.31 ± 0.09	1.47 ± 0.359	0.6924	ns
ICAM1	1.4 ± 0.091	1.73 ± 0.293	0.3252	ns
IL1A	1.95 ± 0.076	1.91 ± 0.177	0.8299	ns
IL6	1.49 ± 0.059	1.7 ± 0.149	0.2282	ns
KLF10	1.09 ± 0.046	1.3 ± 0.108	0.1196	ns
KLF2	1.78 ± 0.062	1.53 ± 0.12	0.1113	ns
KLF3	1.01 ± 0.022	0.7 ± 0.032	<0.0001	****
KLF4	2.87 ± 0.199	1.58 ± 0.254	0.0016	**
LAMC2	1.17 ± 0.031	1.24 ± 0.142	0.6425	ns

MIB1	1.29 ± 0.033	1.16 ± 0.046	0.0432	*
NFKB1	1.02 ± 0.037	0.7 ± 0.059	0.0012	**
NFKBIA	0.89 ± 0.034	1.13 ± 0.102	0.0636	ns
NOTCH2	1.32 ± 0.113	2.62 ± 1.152	0.3123	ns
OCLN	0.94 ± 0.044	0.92 ± 0.095	0.8125	ns
PAPLN	1.5 ± 0.079	1 ± 0.083	0.0004	***
PECAM1	1.07 ± 0.02	0.91 ± 0.032	0.0017	**
PLA2G4A	1.4 ± 0.062	1.51 ± 0.173	0.5597	ns
PLXNA4	1.36 ± 0.207	0.58 ± 0.068	0.0008	***
PROCR	1.24 ± 0.033	0.92 ± 0.033	<0.0001	****
PTGIS	2.05 ± 0.239	1.84 ± 0.442	0.6864	ns
PTGS2	4.92 ± 0.255	6.57 ± 0.422	0.0083	**
S100A10	1.02 ± 0.017	0.82 ± 0.045	0.0051	**
SELE	1.12 ± 0.1	2.66 ± 0.298	0.0025	**
SMAD6	1.74 ± 0.108	1.52 ± 0.178	0.3217	ns
TGFB1	1.14 ± 0.03	1.14 ± 0.065	0.9822	ns
TJP1	0.93 ± 0.022	0.77 ± 0.048	0.0189	*
TNFRSF12A	1.19 ± 0.087	0.84 ± 0.171	0.1105	ns
TSPAN13	1.08 ± 0.033	0.84 ± 0.033	<0.0001	****
TUBB	1.04 ± 0.016	0.9 ± 0.036	0.0091	**
TXNIP	2.76 ± 0.397	0.98 ± 0.18	0.0002	***
VCAM1	1.92 ± 0.14	3.84 ± 0.482	0.009	**

***Supplementary Table 5: var* genotyping of patient-derived isolates after culturing by qPCR.** The primer sets detect multiple group A and A/B *var* domains and have been used to genotype the patient isolates at the time of isolation (original) (Storm et al, ref 26). For the UM and CM-derived isolates, genotyping was performed after a number of days in culture (DIC), as close to the DIC used for the co-culture experiments. The transcript unit (Tu) was calculated per primer set, relative to the transcripts of the endogenous housekeeping genes *seryl-tRNA synthetase* and *aldolase*, and for the combined (sum) CIDRα1 domains. A Tu value of 1 equals low abundance transcript and a value of 32 equals transcript levels as the endogenous housekeeping genes and values ≥32 are highlighted in bold in the dark grey cells. Tu values ≥5 correspond to moderate transcript levels and are highlighted in the light grey cells. Nd: not determined. Receptors for the PfEMP1 domains are listed with names in brackets as probable and left blank when unknown. For a detailed description of the domains see Mkumbaye et al [60].

Domain	**Group**	**Predicted receptor**	**UM1** Original	**UM1** 42 DIC	**UM2** Original	**UM2** 34	**UM3** Original	**UM3** 33 DIC	**UM3** 42	**UM4** Origina	**UM4** 26 DIC
CIDRα1.1	B/A	EPCR	8	1	5	1	2	3	1	5	1
CIDRα1.8a	B/A	EPCR	1	1	1	nd	1	1	1	nd	1
CIDRα1.8b	B/A	EPCR	1	1	1	1	1	1	1	nd	1
Sum: CIDRα1.DC8	B/A	EPCR	8	1	5	1	2	3	1	5	1
CIDRα1.4	A	EPCR	1	1	1	1	1	1	1	1	1
CIDRα1.5a	A	EPCR	1	1	1	1	1	nd	1	1	1
CIDRα1.5b	A	EPCR	4	3	2	1	1	1	1	3	1
CIDRα1.6a	A	EPCR	1	1	1	1	1	1	1	nd	1
CIDRα1.6b	A	EPCR	1	1	1	1	1	nd	1	nd	nd
CIDRα1.7	A	EPCR	4	1	2	1	5	1	1	1	1
Sum: CIDRα1.A	A	EPCR	8	4	4	1	5	1	1	4	1
Sum:CIDRα1_all	A & B/A	EPCR	16	5	8	1	7	3	1	10	1
DBLβ1/3-1	A	ICAM-1	2	1	1	1	1	10	1	5	3
DBLβ1/3-2	A	(ICAM-1)	9	1	3	1	12	17	1	**613**	**341**
DBLβ5	B	ICAM-1	1	1	3	2	1	5	1	2	5
DC5	A	PECAM-1	5	1	1	1	1	1	1	nd	3
CIDRα3.1/3.2	B/C	CD36	5	1	2	1	2	11	1	1	4
CIDRδ	A		2	1	1	1	3	4	2	nd	1
CIDRγ3.1	A		1	1	nd	1	1	1	1	nd	nd
DBLα1all	A		26	3	10	2	7	21	1	**296**	**222**
DBLα2/1.1/1.2/1.4/1.7	A		**36**	5	**33**	11	11	10	2	**109**	**73**
DBLα1.5/1.6/1.8	A	Non-EPCR	20	1	4	1	5	12	2	6	2
CIDRα1.2-K			1	1	nd	1	1	nd	1	nd	nd
CIDRα1.2-K+CIDRα1.3-K			1	1	1	1	1	1	1	nd	1

CM1	CM1	CM1	CM2	CM2	CM3	CM3	CM4	CM4
Original	28 DIC	29 DIC	Original	43 DIC	Original	51 DIC	Original	33 DIC
53	13	1	1	1	no data	1	**52**	2
6	nd	1	nd	1		1	1	1
48	**46**	1	nd	1		1	1	1
107	**59**	1	1	1		1	**52**	2
12	4	1	1	1		1	3	1
33	**53**	1	1	1		1	1	1
1	1	1	2	1		1	7	1
21	11	1	nd	1		1	7	1
1	3	nd	nd	1		1	1	nd
2	23	1	1	1		1	2	1
68	**94**	1	2	1		1	19	1
175	**154**	1	2	1		1	**72**	3
1	**55**	1	1	1		1	6	1
19	**815**	1	1	1		4	1	1
8	9	1	1	1		1	**33**	26
66	**86**	1	nd	1		1	2	1
5	27	1	5	1		1	7	7
8	**44**	1	nd	1		1	3	1
1	1	nd	nd	1		1	1	nd
104	**220**	1	**413**	4		1	**47**	9
185	**383**	4	12	1		5	**156**	14
65	**48**	1	**146**	3		1	**47**	3
1	nd	nd	nd	1		1	1	nd
3	2	1	nd	1		1	1	1

Supplementary Table 6: **Determination of prostaglandin endoperoxide synthase 2 (PTGS2) and prostacyclin production in HBMEC-IE co-cultures by ELISA.** Prostacyclin has a short half-life and therefore its hydrolysis product, 6-keto prostaglandin F1α (6-keto PGF1α), was detected in culture medium after co-culture with IE or RBC. PTGS2 was detected in HBMEC cell lysate after co-culture and calculated as ng PTGS2 per mg total lysate protein. The mean ± SD of 2 technical replicates is shown and per experiment the ratio of the enzyme concentrations for HBMEC-IE and HBMEC-RBC was calculated. 4 UM-derived isolates, 4 CM-derived isolates and SBP1-KO were co-cultured for 6 hours and for the CM4 isolate and SBP1-KO a co-culture of 20 hours was also performed (experiment 12 and 13). As control, HBMEC were incubated with 10 ng/ml TNF for 6 (experiment C2) and 20 hours (experiment C2 and C3). Thrombin is a fast-acting stimulator of prostacyclin production and the concentration of 6-keto PGF1α was detected in HBMEC after 15- and 30-minutes incubation with 5 nM thrombin (experiment C3). Statistical significance between HBMEC-IE and corresponding HBMEC-RBC and or control condition and medium was determined by unpaired t-test with Welch correction with * p-value < 0.05 and ** p-value < 0.01.

		[6ketoPGF1α] pg/ml		[PTGS2] ng/mg protein	
Exp	**Condition**	**Mean ± SD**	**IE/RBC**	**Mean ± SD**	**IE/RBC**
1	6h RBC	608 ± 43			
1	6h UM3-1	996 ± 136	1.64		
1	6h UM3-2	1046 ± 13 *	1.72		
1	6h CM2	1153 ± 271	1.90		
2	6h RBC	1621 ± 390			
2	6h UM1	952 ± 133	0.59		
2	6h CM3	1256 ± 162	0.77		
3	6h RBC	1679 ± 208			

3	6h CM1-1	1505 ± 73	0.90		
3	6h CM1-2	1611 ± 320	0.96		
4	6h RBC	437 ± 38			
4	6h UM2	803 ± 22 *	1.84		
5	6h RBC	664 ± 10		16.2 ± 0.3	
5	6h CM3	358 ± 100	0.54	19.1 ± 1.2	1.2
5	6h UM1	434 ± 56	0.65	10.8 ± 1.7	0.7
6	6h RBC	772 ± 182		18.0 ± 1.0	
6	6h CM4	694 ± 105	0.90	11.4 ± 0.6 *	0.6
7	6h RBC	1309 ± 265		19.0 ± 2.4	
7	6h UM3	1018 ± 79	0.78	10.0 ± 0.2	0.5
8	6h RBC	1194 ± 46		21.0 ± 0.6	
8	6h UM2	5720 ± 1378	4.79	17.4 ± 1.2	0.8
9	6h RBC	396 ± 19		19.4 ± 1.1	
9	6h CM1	695 ± 12 **	1.75	13.2 ± 1.3 *	0.7
10	6h RBC	1595 ± 114			
10	6h UM4	2013 ± 244	1.26		
11	6h RBC	4192 ± 1			
11	6h SBP1-KO-1	7213 ± 561	1.72		
12	6h RBC	1423 ± 109		13.7 ± 0.1	
12	6h CM4	1871 ± 98	1.32	12.5 ± 2.4	0.9
12	20h RBC	3754 ± 170		14.2 ± 1.5	
12	20h CM4	7382 ± 1233	1.97	9.0 ± 1.4	0.6
13	6h RBC	651 ± 11		15.3 ± 0.7	
13	6h SBP1-KO	480 ± 165	0.74	14.4 ± 2.1	0.9
13	20h RBC	2729 ± 113		13.2 ± 1.0	
13	20h SBP1-KO	8526 ± 1295	3.12	11.6 ± 3.1	0.9
C1	30 min medium	100 ± 0			
C1	15 min thrombin (5 nM)	1071 ± 104 *	10.74		
C1	30 min thrombin (5 nM)	826 ± 156	8.29		
C2	6h medium	264 ± 0			
C2	6h TNF (10 ng/ml)	909 ± 62 *	3.44		
C2	20h medium	685 ± 152			
C2	20h TNF (10 ng/ml)	2234 ± 1374	3.26		
C3	20h medium	178 ± 13		123.7 ± 14.9	
C3	20h TNF (10 ng/ml)	1200 ± 70 *	6.73	118.5 ± 19.4	1.0

871

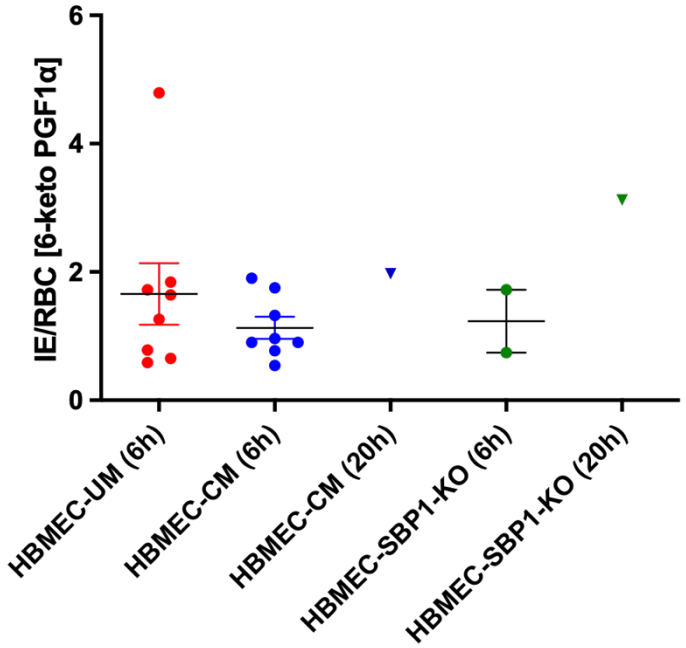

Supplementary Figure 3: **Ratio of 6-keto prostaglandin F1α concentrations in HBMEC-IE and HBMEC-RBC co-cultures.** 6-keto PGF1α was detected in culture medium after co-culture with IE or RBC and per experiment the ratio of the enzyme concentrations for HBMEC-IE and HBMEC-RBC was calculated (data in Supplementary Table 4). Plotted are mean ± SD of the ratios for the co-cultures with CM and UM-derived isolates and the SBP1-KO strain.

Supplementary Table 7: **Production of cytokines and chemokines in HBMEC-IE co-cultures.** A panel of 41 secreted cytokines and chemokines were measured in the co-culture medium of 6 hours co-culture of HBMEC-IE and HBMEC-RBC by Luminex. The results (pg/ml) are shown for 13 cytokines of which the concentration was higher than 5 pg/ml for 3 CM-derived isolates, 2 UM-derived isolates and 2 lab strains: IT4var14 and IT4var37. A positive control of HBMEC activated by 10 ng/ml TNF for 16 hours was included. The mean ± SD of two technical replicates is shown with significance between HBMEC-IE and HBMEC-RBC calculated by unpaired t-test with Welch correction, with * p-value < 0.05, ** p-value < 0.01 and *** p-value <0. 001.The ratio of the values of HBMEC-IE and HBEC-RBC was calculated per experiment. Note that the CM5 isolate was only included in this multiplex experiment and was not part of all the other experiments described.

	G-CSF	GM-CSF	Fractalkine	IFNg	GRO	PDGF-AA	IL-4	IL-6	IL-8	IP-10	MCP-1	RANTES	TNFa
6h RBC	120 ± 10	10 ± 1	165 ± 32	0.7 ± 0.5	567 ± 32	73 ± 5	3.5 ± 2.8	73 ± 60	956 ± 59	1089 ± 212	9162 ± 170	291 ± 22	10.1 ± 0.3
6h CM1	136 ± 10	13 ± 0	102 ± 0	8.0 ± 0.6 **	629 ± 22	85 ± 2	10 ± 4	99 ± 12	1371 ± 13	1209 ± 53	9837 ± 246	686 ± 42 *	10.2 ± 0.5
IE/RBC	1.1	1.2	0.6	10.8	1.1	1.2	2.9	1.4	1.4	1.1	1.1	2.4	1.0
6h RBC	369 ± 30	29 ± 2	341 ± 45	0.7 ± 0.0	2955 ± 108	75 ± 7	44 ± 0	136 ± 12	2293 ± 200	2686 ± 153	10754 ± 457	859 ± 5	15.5 ± 0.7
6h CM4	656 ± 14	49 ± 0.1	219 ± 22	7.4 ± 1.5	4572 ± 167	115 ± 1	55 ± 2	237 ± 3	3764 ± 93	3969 ± 28 *	13028 ± 965	980 ± 22	16.8 ± 1.4
IE/RBC	1.8	1.7	0.6	10.0	1.5	1.5	1.3	1.7	1.6	1.5	1.2	1.1	1.1
6h RBC	423 ± 42	32 ± 0	343 ± 10	1.2 ± 0.4	3167 ± 63	48 ± 3	41 ± 6	128 ± 29	4154 ± 94	1168 ± 22	12360 ± 560	392 ± 23	8.9 ± 0.1
6h CM5	715 ± 6	49 ± 3	161± 13 **	2.9 ± 0.6	3228 ± 197	75 ± 1	47 ± 0.1	170 ± 10	4436 ± 96	1353 ± 92	15720 ±1086	353 ± 343	9.5 ± 0.7
IE/RBC	1.7	1.5	0.5	2.5	1.0	1.6	1.1	1.3	1.1	1.2	1.3	0.9	1.1
6h UM3	805 ± 29	38 ± 2	137 ± 20 *	4.6 ± 0.0 *	2979 ± 143	90 ± 8 *	44 ± 1	155 ± 16	3876 ± 213	1834 ± 60 *	13676 ± 1404	396 ± 12	9.1 ± 0.4
IE/RBC	1.9	1.2	0.4	3.9	0.9	1.9	1.1	1.2	0.9	1.6	1.1	1.0	1.0
6h RBC	151 ± 5	19 ± 1	195 ± 24	1.1 ± 0.0	1308 ± 49	98 ± 7	21 ± 6	117 ± 10	1874 ± 68	1710 ± 30	10297 ± 58	709 ± 99	13.2 ± 0.3
6h UM2	213 ± 1	29 ± 1	107 ± 7	5.4 ± 0.2 *	994 ± 24	92 ± 2	18 ± 7	149 ± 7	2544 ± 77	1869 ± 70	10322 ± 386	666 ± 29	12.6 ± 0.1
IE/RBC	1.4	1.5	0.6	5.0	0.8	0.9	0.9	1.3	1.4	1.1	1.0	0.9	1.0
6h RBC	57 ± 2	9 ± 1	128 ± 7	1.3 ± 0.2	338 ± 3	56 ± 1	1.5 ± 0.0	18 ± 1	1228 ± 8	867 ± 72	7226 ± 366	591 ± 341	21.8 ± 1.5
6h Var37	61 ± 4	9 ± 1	105 ± 11	2.3 ± 0.2	264 ± 12	49 ± 9	5.5 ± 0.0 **	23 ± 4	1529 ± 145	836 ± 73	6240 ± 211	520 ± 40	12.0 ± 0.8
IE/RBC	1.1	1.0	0.8	1.8	0.8	0.9	3.6	1.3	1.2	1.0	0.9	0.9	0.6
6h RBC	212 ± 16	18 ± 0.3	120 ± 11	1.1 ± 0.5	1600 ± 90	50 ± 3	24 ± 0	105 ± 5	1849 ± 38	1262 ± 110	12755 ± 1427	495 ± 7	9.8 ± 0.0
6hVar14	328 ± 22	26 ± 3	71 ± 13	1.6 ± 0.2	1830 ± 235	48 ± 9	29 ± 7	114 ± 18	1972 ± 103	1099 ± 88	12509 ± 1434	460 ± 138	9.9 ± 1.2
IE/RBC	1.5	1.4	0.6	1.5	1.1	1.0	1.2	1.1	1.1	0.9	1.0	0.9	1.0
medium overnight	36 ± 0	1 ± 0.3	23 ± 17	0.4 ± 0	266 ±18	94 ± 16	5.5 ± 0.0	20 ± 2	158 ± 3	12 ± 1	1056 ± 43	1.3 ± 0.4	0.2 ± 0.2
TNF overnight	nd	1385 ± 17 **	2227 ± 25 ***	1.6 ± 0.2	49974 ± 1763 *	138 ± 18	170 ± 6 *	1308 ± 45 *	20734 ± 3283	10465 ± 155 **	13783 ± 1365 *	925 ± 9 **	11068 ± 486 ***
TNF/medium		1372	190	4	188	1.5	31	65	131	864	13	718	52410

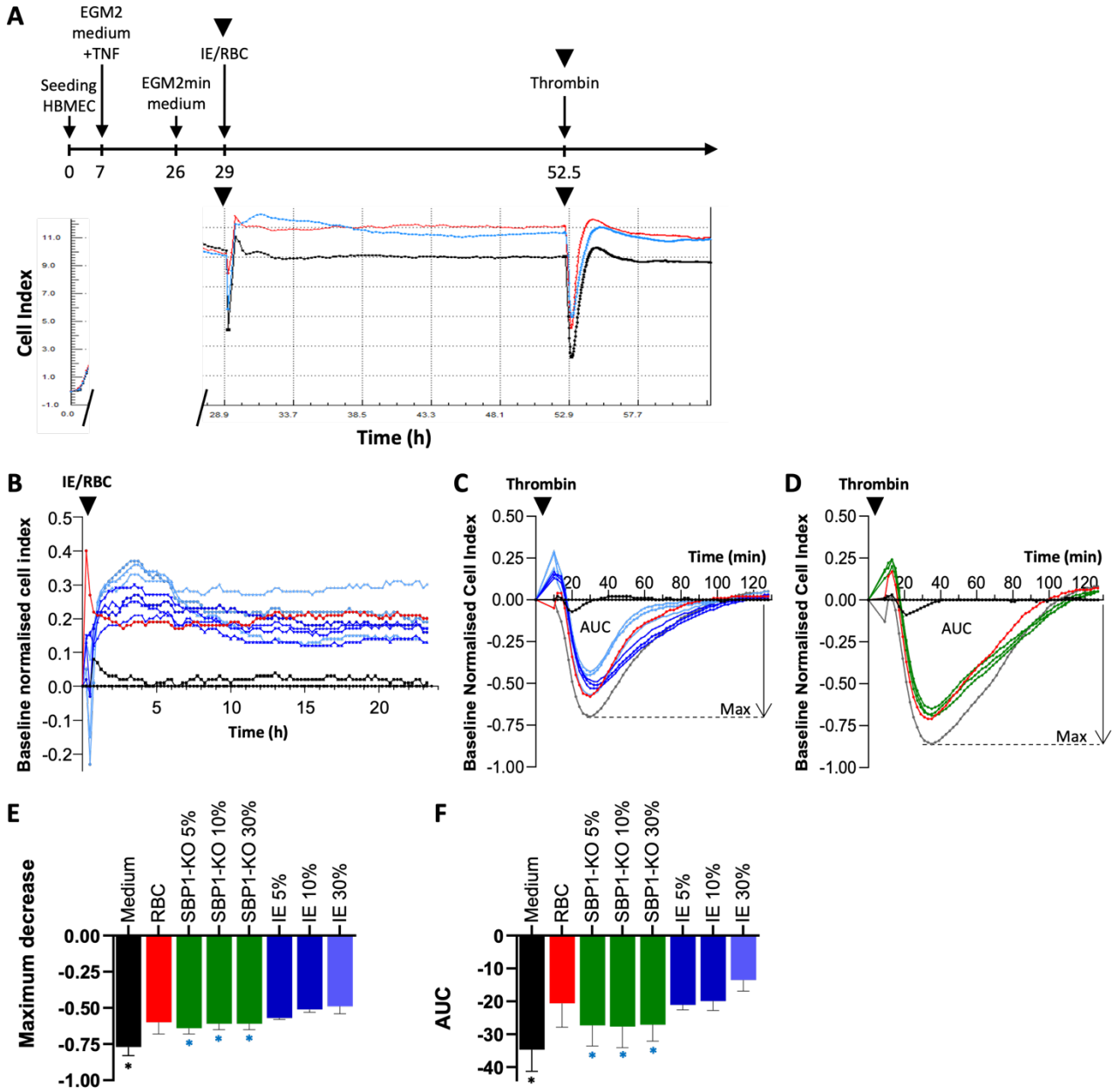

Supplementary Figure 4: **The effect of the patient-derived isolates and SBP1-KO on HBMEC barrier function determined by trans endothelial electrical resistance.** (A) Experimental timeline (not to scale) and a representative cell index trace for IE and thrombin induced changes in HBMEC barrier function. HBMEC were seeded in the E-plate and after approximately 7 hrs the cells were stimulated with 10 ng/ml TNF. The next day, medium was replaced with EGM2min medium and after 2-3 hours, IE at 30% parasitaemia (light blue) or RBC (red), both at 1% HCT, were added. The black line represents medium. After approximately 24 hrs, 5 nM thrombin was added from a concentrated stock solution and cell index was monitored for an additional 10 hours. (B) Cell index trace for the effect of different patient isolates and RBC on HBMEC barrier function of a representative experiment. Cell index was normalised at the time point immediately prior to addition of RBC and IE, indicated by the black triangle, and medium only (black line) was set as baseline. This baseline normalised cell index (BNCI) is shown for 2 UM and 2 CM-derived isolates at 10% parasitaemia (dark blue), 1 UM and 2 CM-derived isolates at 30% parasitaemia (light blue), RBC (red) or replicate medium (black). (C) Thrombin induced decrease in barrier function after 24-hour exposure to patient isolates or RBC. Cell index was normalised at the time point immediately prior to addition of 5 nM thrombin, indicated by the black triangle, and medium without thrombin (black line) was set as baseline. BNCI is shown for medium (dark grey) with the maximum response indicated (max), RBC (red), 1 UM and 2 CM-derived isolates at 30% parasitaemia (light blue) and at 10% parasitaemia (dark blue). (D) As in panel C, but with SBP1-KO at 30% and 10% (green). (E) Maximum decrease of BNCI by thrombin was determined for all co-culture

conditions and mean ± SD are depicted for: control medium (n = 4), RBC (n = 4), SBP1-KO at 5% (n = 3), 10% (n = 3) and 30% parasitaemia (n = 3) and combined patient isolates (IE) at 5% (n = 2), 10% (n = 5) and 30% parasitaemia (n = 5). (F) Area under the curve (AUC) after thrombin induced changes in BNCI was calculated and mean ± SD are depicted for the conditions listed in E. Statistical significance between the various conditions compared to RBC was calculated by unpaired t-test with Welch correction, * p-value < 0.05 (black asterisk). Significance between 30% IE and SBP1-KO was also calculated (blue asterisk).

Supplementary Methods

var Genotyping of Patient-Derived Isolates after Culturing

Genotyping of the isolates after culturing was performed by qPCR using selected primers from a *var* gene primer panel as described by Storm et al [26], with details of the primer design and description of the var domains described by Mkumbaye et al [60]. RNA was isolated from TRIZOL-stored ring stage IE, DNase treated (TURBO™ DNase, Ambion), cDNA synthesised (Tetro cDNA Synthesis Kit, Bioline) and qPCR carried out with SYBR Green PCR Master Mix (QuantiTect, Qiagen). The endogenous housekeeping genes *seryl-tRNA synthetase* and *aldolase* were used to determine the relative levels of *var* transcripts using the formulae ΔCt *var*-primer = Ct *var* primer minus Ct average of endogenous primers. The transcript unit (Tu) was then calculated as $Tu = 2^{(5-\Delta Ct\ var\text{-}primer)}$. Any low abundance transcripts with a ΔCt *var*-primer >5 was assigned a value of 5, thus subsequently a Tu value of 1. A Tu value of 32 equates to equal transcript levels as the endogenous control genes [60]. The Tu of the patient isolates at the time of isolation from peripheral blood was determined previously [26].

Preparation of HBMEC-IE Co-culture Samples for Phenotypic Analysis

After 6 or 20 hour co-culture with patient isolates, SBP1-KO, RBC or additional controls, co-culture medium was collected, centrifuged for 5 min at 900 g to remove IE, RBC or cellular debris and the supernatant frozen at -80 °C. For cell lysates, HBMEC were washed twice with warm EGM2 medium without supplements and lysed in 50 µl lysis buffer (RIPA buffer (Sigma, R0278) with HALT™ protease inhibitor cocktail (Thermo Scientific, 78429) for 10 minutes on ice. The lysed cells were transferred from the well into a tube, placed on ice for an additional 25 minutes, centrifuged for 5 min at 13,000 g at 4 °C and the supernatant frozen at -80 °C.

Determination of the Concentrations of Prostacyclin and Prostaglandin Endoperoxide Synthase 2

Prostacyclin has a short half-life and therefore its hydrolysis product, 6-keto prostaglandin F1α (6-keto PGF1α), was detected in co-culture medium by competitive ELISA according to the manufacturer's instructions (Cayman Chemicals, 515211). The four UM and four CM-derived isolates and SBP1-KO were co-cultured for 6 hours with their respective RBC as control. The CM4 isolate and SBP1-KO were also co-cultured for 20 hours. As additional controls, HBMEC were incubated with 10 ng/ml TNF for 6 and 20

962 hours and with 5 nM thrombin for 15 and 30 minutes. Co-culture medium of two independent 6 hour co-
963 culture experiments with the patient isolates, except UM4 and CM2, and SBP1-KO were used, and all
964 samples were measured in duplicate using 2 ELISA plates on the same day. All samples were diluted 2
965 times, but the 20 hour TNF stimulation sample was diluted 5 times. The concentration of 6-keto PGF1α
966 was calculated using the provided standards.
967
968 Prostaglandin endoperoxide synthase 2 (PTGS2) was detected in HBMEC cell lysate by ELISA according
969 to the manufacturer's instructions (Reddot, RD-PTGS2-Hu). Lysates were diluted 5 times and for duplicate
970 samples the concentration of PTGS2 was calculated using the provided standards. On the same day, total
971 protein concentration of the lysates was determined with the BCA kit (Biorad, 5000002) with BSA as
972 standard and ng PTGS2 per mg total protein calculated.
973
974 **Detection of Cytokines and Chemokines**
975 A panel of 41 secreted cytokines and chemokines was measured in the co-culture medium of 6 hours co-
976 culture of HBMEC-IE, HBMEC-RBC and controls using the human cytokine/chemokine 41 plex
977 Immunology Multiplex Assay according to the manufacturer's instructions (Merck, HCYTMAG-60K-
978 PX41). In addition to three CM and two UM-derived isolates, two lab strains, IT4var14 and IT4var37, and
979 a positive control of HBMEC activated by 10 ng/ml TNF for 16 hours were included. The panel included:
980 sCD40L, Eotaxin, FLT-3L, Fractalkine, G-CSF, GM-CSF, GROα, IFNα2, IFNγ, IL-1α, IL-1β, IL-1RA,
981 IL-2, IL-3, IL-4, IL-5, IL-6, IL-7, IL-8, IL-9, IL-10, IL-12 (p40), IL-12 (p70), IL-13, IL-15, IL-17A, IL-
982 17E/IL-25, IL-17F, IL-18, IL-22, IL-27, IP-10, MCP-1, MCP-3, M-CSF, MDC, MIG, MIP-1α, MIP-1β,
983 PDGF-AA, PDGF-AB/BB, RANTES, TGFα, TNFα, TNFβ, VEGF-A.
984
985 **Measuring HBMEC Barrier Integrity**
986 Barrier function was measured by real time Trans Endothelial Electrical Resistance (TEER) analysis with
987 the xCELLigence® RTCA S16 system (ACEA Biosciences). HBMEC cells were seeded at 50,000
988 cells/cm^2 (1x10^4 cells) in Attachment Factor coated E-Plates 16 PET (ACEA Biosciences) in EGM2
989 medium and the arbitrary cell index (CI) was recorded. After approximately 7 hrs the medium was replaced
990 with EGM2 medium with 10 ng/ml TNF and the next day, medium was replaced with EGM2min medium.
991 IE suspensions at 30%, 10% or 5% parasitaemia were prepared at 1% HCT in EGM2min medium and the
992 medium in the E-plate replaced with 100 µl suspension, equivalent to 3x106, 1x106 and 0.5x106 IE,
993 respectively. RBC at 1% HCT and medium only were used as control.
994 After approximately 24 hrs, 5 nM thrombin was added from a concentrated stock solution and cell index
995 was monitored for an additional 10 hours, starting at 2 minute intervals. For analysis, the cell index was

996 normalised either at the time point immediately prior to addition of IE or thrombin (normalised cell index)
997 and medium only was set as baseline (baseline normalised cell index, BNCI). To determine the effect of
998 thrombin, the maximum decrease in BNCI and the area under the curve after recovery to baseline was
999 calculated.